

# REPORT DOCUMENTATION PAGE

AFRL-SR-AR-TR-04-

Public reporting burden for this collection of information is estimated to average 1 hour per response, including the time for reviewing instructions, searching existing data sources, gathering the required data, reviewing existing materials, completing the collection of information, Send comments regarding this burden estimate or any other aspect of this collection of information, including suggestions for reducing the burden, to Washington Headquarters Services, Directorate for Information Operations and Reports, 1215 Jefferson Davis Highway, Suite 1204, Arlington, VA 22202-4302, and to the Office of Management and Budget, Paperwork Reduction Project (0704-0188), Washington, DC 20503.

0096

1. AGENCY USE ONLY (Leave blank)		2. REPORT DATE February 2004		3. REPORT TYPE AND DATES COVERED Final Report (1 Nov 99 - 31 Oct 03)	
4. TITLE AND SUBTITLE BREAKTHROUGH TO OPTIMIZED PLASMA THRUSTERS				5. FUNDING NUMBERS F49620-00-1-0032 2308/AX 61102F	
6. AUTHOR(S) Dr. Thomas York					
7. PERFORMING ORGANIZATION NAME(S) AND ADDRESS(ES) The Ohio State University Dept of Aerospace Engineering, Applied Mechanics, and Aviation 328 Bolz Hall, 2036 Neil Avenue Columbus, OH 43210-1276				8. PERFORMING ORGANIZATION REPORT NUMBER	
9. SPONSORING/MONITORING AGENCY NAME(S) AND ADDRESS(ES) AFOSR/NA 4015 Wilson Blvd., Room 713 Arlington, VA 222301-1954 Program Manager: Dr. Mitat Birkan				10. SPONSORING/MONITORING AGENCY REPORT NUMBER	
11. SUPPLEMENTARY NOTES					
12a. DISTRIBUTION AVAILABILITY STATEMENT Approved for public release, distribution unlimited					
13. ABSTRACT (Maximum 200 words) Analytic models predict the possibility of extending the range of performance parameters of Pulsed Plasma Thrusters (PPT) by using propellants other than the traditionally used Teflon. A theoretical and experimental effort was initiated at The Ohio State University to investigate the use of alternative propellants for PPT. Analytical and numerical calculations (MACH2) indeed indicate a significant broadening of the obtainable range of specific impulse and thrust-to-power ratios when alternative propellants such as lithium or water are utilized. Consequently, in an effort to investigate changes in physical phenomena and thruster performance experimentally, a hybrid thruster was designed and built, facilitating the use of alternatively water or Teflon. The thruster design includes a unique water propellant feed system, allowing the supply of the water propellant without detrimentally affecting the inherent simplicity of the PPT system. The thruster operation and performance was investigated by several different diagnostic methods, including current and voltage measurements, Langmuir probes, and magnetic field probes. Furthermore, impact pressure measurements in the plume of the thruster allowed new insight into the plume structure and the accurate evaluation of impulse bits. Employment of the diagnostic methods for Teflon and water propellant enabled the unambiguous identification of propellant related effects such as reduced electron temperature and higher exhaust velocities in the case of water propellant.					
14. SUBJECT TERMS				15. NUMBER OF PAGES 68	
				16. PRICE CODE	
17. SECURITY CLASSIFICATION OF REPORT U		18. SECURITY CLASSIFICATION OF THIS PAGE U		19. SECURITY CLASSIFICATION OF ABSTRACT U	
20. LIMITATION OF ABSTRACT					

20040220 315


BREAKTHROUGH TO OPTIMIZED PULSED PLASMA THRUSTERS

FINAL REPORT

under  
Air Force Office of Scientific Research  
Grant No. F49620-00-1-0032  
OSU RF #738668

\*\*\*

Start Date: November 5, 1999  
End Date: November 31, 2003

Report submitted by:  
(PI) Thomas M. York 

February 12, 2004  
Aerospace Engineering and Aviation Department  
The Ohio State University  
Columbus, Ohio 43210

Approved for public release,  
distribution unlimited

## SUMMARY OF ACTIVITIES

### Modeling and Predictions of Performance:

The work carried out under this grant took as its starting point results from previous work which predicted performance of PPT thrusters based on computational and analytic models. Each of these models showed that by using propellants other than Teflon, increases in Thrust/Power and /or Specific Impulse were possible. For some alternate propellants, predictions from these models were not in agreement, actually in opposition. The results of this work are described in the 1999 paper. Accordingly, the breakthrough to improved performance would have to be determined by experiment.

### Alternate Propellant Selection:

The range of possible propellants that could replace Teflon is not that extensive due to practical considerations. Candidates examined included Cesium, Lithium and Water. Practical operational difficulties with cesium and lithium ruled them out, but water not only was practical, it has exceptional advantages in potential availability in space and on space missions. Interestingly, predictions for performance with water were significantly different in each model prediction.

### Experimental Findings:

To conduct these experiments with the high accuracy desired, a new facility was designed and constructed using available components in the laboratory of the PI (T. M. York replaced P. Turchi before the start of contract work). So this was a no-cost improvement to the originally proposed effort. Also, all diagnostics used were developed and available from the new PI Laboratory, again enhancing the effort.

The new vacuum facility provided substantially improved ambient vacuum conditions

A new precise, controlled water injection system was successfully developed.

A new thruster was constructed that allowed Teflon propellant and water propellant to be tested in the same device. This thruster also had significantly lower inductance which resulted in higher performance even for the Teflon thruster.

Important new measurements were made of impact pressure in the exhaust flow of the Teflon and water propellant thrusters. Pressure is directly related to momentum flux, the most important variable in a thruster. These were coordinated with measurements from Langmuir probes (electron density) and magnetic probes (Magnetic pressure and current density). The time histories showed important differences between water and Teflon, with little of a secondary thermal ejection of propellant in water.

To provide critical data on actual thrust performance, the Teflon thruster was taken to NASA Glenn Research Center (Cleveland, Ohio) and during a two-day period thrust measurements were made. These have proven to be invaluable in coordinating with local probe measurement, especially impact pressure in the exhaust. There has been a failure to secure further facility availability at NASA Glenn to conduct the all important thrust measurements on the water thruster. Also, attempts to schedule thrust stand measurement at Air Force (RL) facilities have also met with failure to this point. Apparently, any plan to make such tests will have to be abandoned.

The experimental results show that the water thruster operates with almost 100% electromagnetic acceleration of propellant, a long sought after goal. This manifests itself in much higher Specific Impulse and Efficiency for the water propellant thruster.

The correlation of the experimental data with the computational and analytic models is not good. Obviously, further work would be needed in order to create more reliable predictors of thruster performance.

Based on the above summary of findings during this research effort, the goal of achieving breakthrough to optimized pulsed plasma thrusters has been achieved within the constraints of the grant agreement.



## DOCUMENTATION OF RESEARCH RESULTS

On the following pages, the cover page, Abstract and sections of the thesis that provide a summary of the findings of a Ph. D. thesis that was completed under the support of this Grant are presented.

Carsten Scharlemann, Ph. D. Thesis (Dec.) 2003

Following the thesis material, a series of research papers presented at technical conferences are presented. These comprise the bulk of the product of this research. They are as follows:

AIAA 00-3260	Scharlemann, Corey, I. Mikellides, Turchi, P. Mikellides
AIAA 02-4270	Scharlemann, York, Turchi
IEPC 03-112	Scharlemann, York
AIAA 2003-5022	Scharlemann, York
AIAA 2003-5023	Scharlemann, York

PERSONNEL EXPENDITURES-  
(Without Fringe and Overhead)

Staff and Student Support

<u>Individual</u>	<u>Position</u>	<u>Expend.(approx.)</u>	<u>Degree</u>
Thomas York	PI	\$16.7K	
Carsten Scharlemann	GRA	.\$66.3K	PhD
Tomokazu Umeki	GRA	\$ 3.4	PhD
Trenton White	UG	\$ 2.6	B.S.

With added Overhead and Fringe (Non students) , Total for salaries was: \$153 K

# INVESTIGATION OF THRUST MECHANISMS IN A WATER FED PULSED PLASMA THRUSTER

## DISSERTATION

Presented in Partial Fulfillment of the Requirements for  
The Degree Doctor of Philosophy in the Graduate  
School of The Ohio State University

By

Carsten A. Scharlemann

\*\*\*\*\*

The Ohio State University  
2003

Dissertation Committee:

Professor Thomas M. York, Adviser

Professor Michael G. Dunn

Professor James N. Scott

Approved by

---

Adviser

Aeronautical and Astronautical  
Engineering Graduate Program

## ABSTRACT

Analytic models predict the possibility of extending the range of performance parameters of Pulsed Plasma Thrusters (PPT) by using propellants other than the traditionally used Teflon. A theoretical and experimental effort was initiated at The Ohio State University to investigate the use of alternative propellants for PPT. Analytical and numerical calculations (MACH2) indeed indicate a significant broadening of the obtainable range of specific impulse and thrust-to-power ratios when alternative propellants such as lithium or water are utilized. Consequently, in an effort to investigate changes in physical phenomena and thruster performance experimentally, a hybrid thruster was designed and built, facilitating the use of alternatively water or Teflon. The thruster design includes a unique water propellant feed system, allowing the supply of the water propellant without detrimentally affecting the inherent simplicity of the PPT system.

The thruster operation and performance was investigated by several different diagnostic methods, including current and voltage measurements, Langmuir probes, and magnetic field probes. Furthermore, impact pressure measurements in the plume of the thruster allowed new insight into the plume structure and the accurate evaluation of impulse bits. Employment of the diagnostic methods for Teflon and water propellant enabled the unambiguous identification of propellant related effects such as reduced electron temperature and higher exhaust velocities in the case of water propellant.

The electromagnetic nature of the water thruster was clearly identified. For 30 J discharge energy, the water thruster requires only 5% of the mass of a Teflon thruster to produce an impulse of 30% of the magnitude of the Teflon thruster, suggesting greatly increased propellant efficiencies. In agreement with the plasma diagnostic results, a specific impulse for the water thruster of up to 8000 s and efficiencies of up to 16% were evaluated.

## 9.8 Performance Evaluation and Comparison with the Analytic and Numerical Models

Thruster performance can be evaluated with the mass bit known from Chapter 7 and the above presented impulse bit values based on the impact pressure measurements.

The following standard equations are utilized to calculate the specific impulse  $I_{sp}$  and efficiency  $\eta$ :

$$I_{sp} = \frac{I_{bit}}{\bar{m}_{bit} \cdot g} \quad (9.17)$$

$$\eta = \frac{I_{bit}^2}{2 \cdot E \cdot \bar{m}_{bit}} \quad (9.18)$$

with earth's gravitational acceleration,  $g = 9.81 \text{ m/s}^2$ , the discharge Energy,  $E$ , and the average mass bit,  $\bar{m}_{bit}$ . The results of these calculations are summarized in Table 9.6.

In general, the performance parameters for the thruster using Teflon compare very well to similar thruster types. For comparison, the EO-1 has a specific impulse of 1400 s at 56 J discharge energy with a thruster efficiency of 8%. The unusually low ablation rate for the 10 J case is attributed to an observed slight carbonization of the Teflon ablation surface (see Chapter 7).

The specific impulse and the efficiencies for water are several factors higher than for Teflon. This result is attributed to a more efficient coupling of energy into the plasma, the lower average mol weight for water (6g/mol) compared to the average mol weight of Teflon (31 g/mol), and to the controlled supply of the mass bit in the case of the water

thruster, avoiding therefore the significant late time mass losses inherent in Teflon thrusters.

The impulse bit values given in Table 9.6 are based on the impulse bit measurements and the correction factor calculated for Teflon (Chapter 9.5). As outlined in Chapter 9.6, the higher Mach number for the water case indicates a higher correction factor for water. This would imply that the impulse bit values for water, as given in Table 9.6, underestimate the correct value.

Discharge energy [J]	Impulse bit, GRC [ $\mu\text{N}\cdot\text{s}$ ]		Impulse bit, Pressure probe [ $\mu\text{N}\cdot\text{s}$ ]		Mass bit [ $\mu\text{g}/\text{discharge}$ ]		Specific impulse [s]		Efficiency	
	Teflon	Water	Teflon	Water	Teflon	Water	Teflon	Water	Teflon	Water
10	122	—	124	47	11.9	$\sim 1.64$	1060	2920	6.5	6.7
20	273	—	281	90	27.5	$\sim 1.64$	1040	5600	7.2	12.3
30	440	—	440	128	35.3	$\sim 1.64$	1270	7960	9.1	16.6

Table 9.6: Thruster performance for the water and Teflon mode

Fig. 9.12 summarizes the thrust-to-power ratios for the Teflon and water thruster as a function of the specific impulse as predicted by MACH2, the analytic model, and those found experimentally. Also included is the degree of ionization as predicted by MACH2 and assumed by the analytic model respectively.

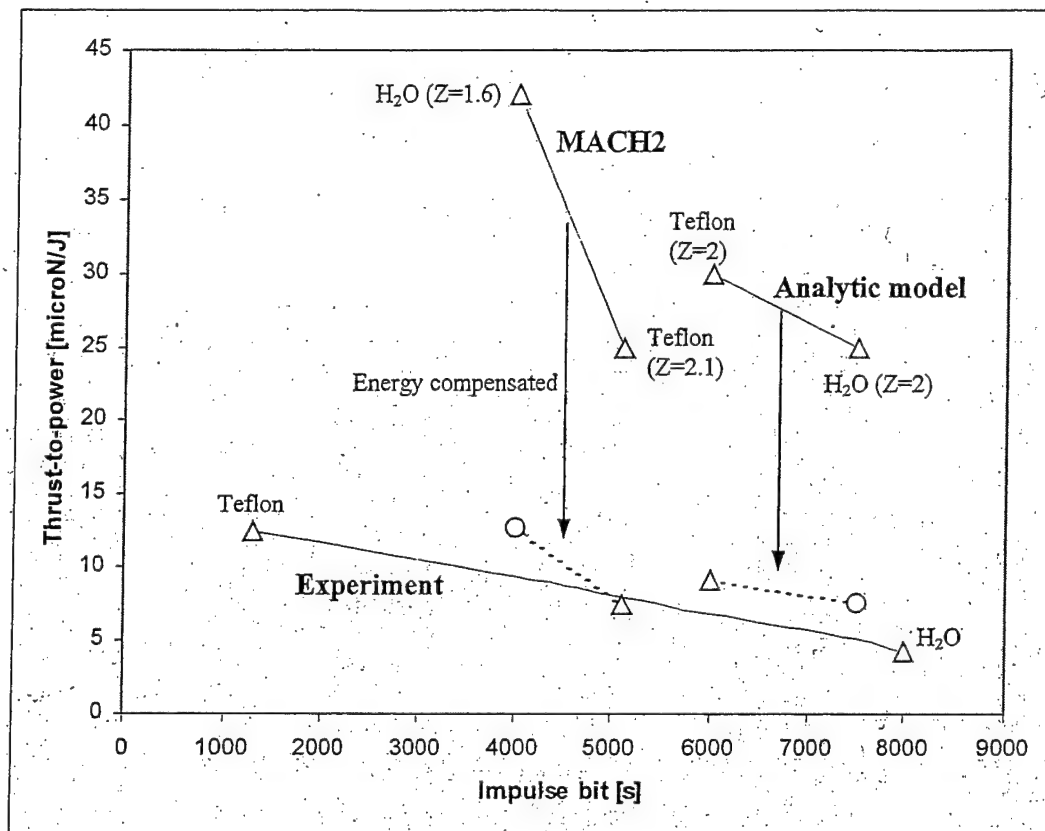


Fig. 9.12: Comparison of thrust-to-power ratios prediction from MACH2 and the idealized analytic model with experimental results

Certain important “operational” conditions in the theoretical calculations, such as discharge energy and current waveform, differ significantly from those present in the experiments. For example, while the discharge energies for the experiments in the present work varied between 10 and 30 Joules, they were in excess of 100 Joules for the MACH2 and the analytic model calculations. However, exploiting the linear dependency of the thrust-to-power ratios to the discharge energy, the results from the analytic and numeric calculations can be scaled down to the energies present in the experiment (see Fig. 9.12)



The experimental values for water and Teflon show an anticipated trend, namely higher specific impulse for the lower average molecular weight propellant. A comparison between the specific impulse values for water and Teflon demonstrates the potential of the water fed Pulsed Plasma Thruster. Water shows an improvement in specific impulse of more than a factor 6 compared to the Teflon case. This translates into a significant reduction of the required amount of propellant or, alternatively, into an increase of lifetime expectancy for a satellite system.

The results from MACH2 and the analytic model agree with each other for Teflon, but not for water. As discussed earlier, this is partially attributed to the inadequacy of assumptions made in the development of the analytic model (see discussion in Chapter 4). The high thrust-to-power ratio/low specific impulse predicted by MACH2 for water in comparison to that for Teflon might be attributed to the numerical modeling of the propellant feed. MACH2 models the water "ablation" in a fashion similar to the case of Teflon, only with different material properties.

As mentioned above, a comparison between both the numerical and analytic results with the experimental ones is complicated by significantly different conditions. A more detailed and accurate comparison between experimental results and those predicted by MACH2 would require changing the input parameters for MACH2, such as the discharge current waveform and discharge energy, to match the present experiment.

## 9.9 Summary

A comprehensive investigation of a Pulsed Plasma Thruster using water as propellant has been conducted. The dominant acceleration processes were identified and compared to a thruster using the traditional Teflon propellant. Magnetic field measurements have proven the electromagnetic nature of the PPT using water. By employing an impact pressure probe, the impulse bit of the water PPT was evaluated. The accuracy of this unique method was verified with a Teflon thruster by comparing impulse bit measurements conducted on a thrust stand at the NASA Glenn Research Center with the impulse bit derived from impact pressure measurements in the plume. These measurements again confirm the electromagnetic nature of the water PPT.

It was found that the observed lower discharge currents for the water thruster, in comparison with the Teflon thruster, are due to a decrease in plasma conductivity. However, in spite of the lower discharge currents, it was shown that the exhaust velocities for the water thruster exceeded those of the Teflon thruster. Evaluation of the rate of change in magnetic field and the associated current density has shown that the current sheet in the case of the water thruster has significant higher velocities, explaining the observed higher exhaust velocities. A comparison of the energy deposited into resistive heating of the plasma for water and Teflon showed that much more energy per unit mass of propellant is utilized for means of acceleration in the case of water, explaining partially the experimentally evaluated higher exhaust velocities.

The following simple calculation demonstrates the improved propellant utilization efficiency of the water thruster: the indicated peak exhaust velocities for Teflon and water

are on average around 50 km/s and 80 km/s, respectively. Using these velocities and the evaluated impulse bits, one can evaluate the mass bits necessary to produce the observed impulse bit. For Teflon (30 J discharge energy) this results in a necessary mass bit of  $9\mu\text{g}/\text{discharge}$ . This is only 25% of the total mass loss per discharge, a result which correlates well with estimates, made previously<sup>9</sup> and indicates poor propellant utilization efficiency. On the other hand, repeating this calculation for water, one obtains a value of  $2\mu\text{g}/\text{discharge}$ , agreeing well with the measured mass flow of  $1.64\mu\text{g}/\text{discharge}$  and indicating therefore vastly improved propellant utilization efficiency.

A performance evaluation for the water thruster was conducted and compared with the thruster using Teflon as propellant. A significant increase in specific impulse, combined with efficiencies nearly a factor of 2 higher than for the Teflon thruster, emphasizes the potential of water as propellant for Pulsed Plasma Thrusters in general and the value of the developed water PPT in particular.

## CHAPTER 10

### CONCLUSIONS

Experimental efforts were initiated to investigate physical phenomena and the performance of a Pulsed Plasma Thruster utilizing water as propellant. A hybrid Pulsed Plasma Thruster was designed, fabricated, and subsequently investigated. This thruster type can utilize alternatively water or Teflon without major changes in thruster geometry or circuitry.

A unique propellant feed system was developed in order to supply the discharge with the necessary amount of propellant. The feed system employs a Passive Flow Control (PFC) concept based on the diffusion of the water propellant through a porous ceramic inlay. Studies have been performed to investigate different porous materials with regard to their suitability and the influence of their geometry on the obtained mass flow rate.

Synchronization issues between triggering the main discharge and supplying the propellant were avoided by supplying the water into the vicinity of the spark plug, from where it is delivered into the acceleration channel upon triggering the spark plug.

Extensive diagnostics were performed to investigate unambiguously the influence of utilizing water as propellant for a PPT by direct comparison of the measurement results obtained for Teflon with those obtained with water.

A unique method to evaluate the impulse bit of the PPT by measuring the impact pressure in the plume was developed. The accuracy of this method was verified by direct comparison with impulse bits measured on a thrust stand at the NASA Glenn Research Center. Magnetic field measurements and the performed analytics have clearly shown that the water thruster is indeed an electromagnetic thruster. Time-of-Flight measurements employing Langmuir probes and pressure probes have shown that the velocity of the expelled water plasma is a factor of 1.5 to 2 higher than observed in the Teflon case, although the discharge currents in the water case are around 40% lower.

Evaluation of the plasma conductivity disclosed the reason for the low discharge currents inherent in the water thruster: the water discharge exhibits a plasma conductivity about a factor of 3 - 4 lower than in the case of Teflon. The reasons for the lower conductivity are yet unknown and require further investigation.

In spite of the lower discharge currents, the measurements of all the employed diagnostic methods show consistently higher exhaust velocities obtained with water in comparison with Teflon, due to a more efficient deposition of energy into kinetic energy. This, along with the apparent prevention of late time mass losses, results in a superior performance of the water-fed Pulsed Plasma compared to a Teflon thruster.



**AIAA-00-3260**

**PULSED PLASMA THRUSTER VARIATIONS  
FOR IMPROVED MISSION CAPABILITIES**

C.A. Scharlemann, R. Corey, I.G. Mikellides, P.J. Turchi and P.G. Mikellides  
The Ohio State University  
Columbus, OH

**36<sup>th</sup> AIAA/ASME/SAE/ASEE Joint Propulsion Conference & Exhibit  
16-19 July 2000, Huntsville, Alabama**

For permission to copy or to republish, contact the American Institute of Aeronautics and Astronautics,  
1801 Alexander Bell Drive, Suite 500, VA, 20191-4344

# PULSED PLASMA THRUSTER VARIATIONS FOR IMPROVED MISSION CAPABILITIES

C.A. Scharlemann\*, R. Corey<sup>#</sup>, I.G. Mikellides<sup>+</sup>,  
P.J. Turchi<sup>++</sup>, P.G. Mikellides<sup>\*\*</sup>

The Ohio State University  
Columbus, Ohio

## Abstract

An idealized model in conjunction with simple numerical analysis has been developed to provide physical insights and guidance toward design of consistently efficient PPTs. In addition, the model proposes directions for expanding the PPTs mission capabilities by proper propellant variations. The magnetohydrodynamics code MACH2 has been utilized to refine the aforementioned insights. Four different propellants - Teflon<sup>®</sup>, water, lithium and cesium - were examined under optimal current waveforms that will minimize the well-known mass inefficiencies. The analysis shows that indeed, the concept of propellant variations offers a wider envelope of available Thrust-to-Power ratios and thus a higher level of mission applicability for the pulsed plasma thrusters.

## Introduction

The well known advantages of pulsed plasma thruster (PPT), like its simplicity, robustness and ability to operate in the low energy regime are counterbalanced by its very low efficiency. This efficiency degradation has been attributed to poor propellant utilization in conjunction with non-optimal circuit design<sup>1</sup>. Specifically, post-pulse mass losses are substantial and

since they escape with low thermal speeds they decrease the overall specific impulse and thrust efficiency. In order to improve the PPT's efficiency and expand its mission capabilities, this late mass loss needs to be eliminated and design directions for variable thrust-to-power ratios needs to be proposed. A recently developed idealized model (IM), describing the ablation and acceleration processes in a PPT, in conjunction with a model for the production of late time masses is utilized to guide such directions<sup>2</sup>.

One possibility to gain a broader range of thrust-to-power ratio and therefore increase the mission capabilities of PPTs is the use of propellants other than Teflon<sup>®</sup>. The idealized model was used to find the optimum current wave form in terms of magnitude and pulse duration for four different propellants: Teflon<sup>®</sup>, Water, Lithium, Cesium. Using the results of the idealized model, a full blown magnetohydrodynamic code, MACH2<sup>3,4</sup>, was used for verification.

## Idealized model

For easier accessible solutions of the ablation and acceleration processes in PPTs, an idealized model was developed. The core of this model is the assumption of the existence of two distinguished points in the flow of a PPT: A sonic point, adjacent to the propellant surface and a magnetosonic point further downstream. By assuming a one-dimensional quasi-steady plasma flow with low ratios of thermal to magnetic pressure, (low  $\beta$ ), it can be shown that a point in the flow, called the magnetosonic point, exists where the flow velocity equals Alfven's wave speed given by

\*Graduate Research Assistant, The Ohio State University, Member DGLR,

<sup>#</sup> Graduate Research Assistant, The Ohio State University,

<sup>+</sup> Graduate Research Assistant, The Ohio State University,

<sup>++</sup> Adjunct Professor/Senior Research Scientist, Los Alamos National Laboratory, Senior Member AIAA

<sup>\*\*</sup> Adjunct Assistant Professor, The Ohio State University, Member AIAA

Copyright© 2000 by Carsten A. Scharlemann. Published by the American Institute of Aeronautics and Astronautics, Inc. with permission

$$u^* = v_A = \frac{B^*}{\sqrt{\mu \cdot \rho^*}} \quad (1)$$

with the density  $\rho$ , and the magnetic field  $B$ . Starred quantities refer to the magnetosonic point. Under the assumptions stated above, the conservation of mass, momentum and energy can be written like

$$\begin{aligned} \dot{m} &= \rho^* \cdot u^* \cdot A \\ \dot{m} \cdot \frac{du}{dx} &= j_y \cdot B_z \cdot A \\ \dot{m} \left( h + u \frac{du}{dx} \right) &= - \frac{E \cdot A}{\mu} \cdot \frac{dB_z}{dx} \end{aligned} \quad (2)$$

with the flow velocity  $u$ , the specific enthalpy  $h$ , the current density  $j$ , the constant channel area  $A$ , the constant electric field  $E$ , and  $x$  as the direction of the flow. Substituting  $B_z$  - given by Ampere's law - into the equation for conservation of momentum and integrating from stagnation point to the magnetosonic point results in an expression for the mass flow

$$2 \cdot \mu \cdot \dot{m} \cdot u^* = A (B_o^2 - B^{*2}) \quad (3)$$

Further substitution of the mass flow rate, given by the conservation of mass, into eq.(3) shows the following proportionality between the magnetic fields at the magnetosonic point and at the stagnation point:

$$\frac{B^*}{B_o} = \frac{1}{\sqrt{3}} \quad (4)$$

where the index (o) refers to quantities at the stagnation point. Combining this proportionality with eq.(2) and with the flow velocity given by eq.(1), gives the mass flow rate due to the magnetosonic condition as

$$\dot{m} = \frac{A \cdot B_o^2}{3 \cdot \mu \cdot u^*} = \frac{A \cdot \mu \cdot j^2}{3 \cdot d^2 \cdot u^*} \quad (5)$$

with the discharge current density  $j$  and  $d$  the gap between the electrodes. Integrating the conservation equation of energy from the stagnation point to the magnetosonic point results in

$$\dot{m} \cdot h_o + \frac{A(E \cdot B)_o}{\mu} = \dot{m} \left( h^* + \frac{u^{*2}}{2} \right) + \frac{A(E \cdot B)^*}{\mu} \quad (6)$$

In the additional limit of high magnetic Reynolds numbers at the magnetosonic point, we can write for the magnetosonic velocity

$$u^* = \sqrt{\frac{h^* - h_o}{\sqrt{3} - 1.5}} = 1.468 \sqrt{2 \Delta h} \quad (7)$$

Since

$$h^* - h_o = \Delta h \cong c_p \cdot T^* + (\epsilon_i)^* \quad (8.1)$$

and if we assume that energy deposition to ionize dominates contribution to the thermal internal energy and  $p(dv)$ - work, i.e.

$$c_p \cdot T^* \ll \epsilon_i \quad (8.2)$$

then  $u^*$ , the speed at the magnetosonic point, tends to remain fixed and proportional to Alfven critical speed

$$u_{crit} = \sqrt{2 \cdot \epsilon_i} \quad (9)$$

and

$$u^* = 1.468 \cdot u_{crit} \quad (10)$$

We can therefore rewrite the mass flow rate

$$\dot{m} = \frac{\mu \cdot j^2}{4.404 \cdot d^2 \cdot u_{crit}} \quad (11)$$

Equation (11) implies that the mass flow rate, based on the magnetosonic condition, is a function of the material properties, the thruster geometry and the operating current level.

Similarly, we can express the mass flow rate in terms of conditions at the thermal sonic point adjacent to the propellant surface. Assuming steady state flow of an ideal gas, the mass flow rate based on sonic conditions can be written as a function of the pressure  $p_a$  and temperature  $T_a$  at the sonic point

$$\dot{m} = A \cdot p_a \cdot \sqrt{\frac{\gamma}{R \cdot T_a}} \quad (12)$$

where  $R$  is the specific gas constant. The conservation of momentum and energy relates the surface pressure  $p_s$  and surface temperature  $T_s$  to the condition at the sonic point with

$$p_a = \frac{p_s}{1 + \gamma} \quad (13)$$

$$T_a = \frac{2 \cdot T_s}{1 + \gamma} \quad (14)$$



Substituting eq. (13) and (14) into eq.(12), and setting the surface pressure equal to the equilibrium vapor pressure results in an expression for the mass flow rate based on the sonic point assumption

$$\dot{m} = A \cdot p_{eq} \sqrt{\frac{\gamma}{2(1+\gamma)R \cdot T_s}} \quad (15)$$

with

$$p_{vap} = C_1 \cdot e^{\frac{C_2}{T_s}} \quad (16)$$

where  $C_1$  and  $C_2$  are material dependent constants that can be found empirically. By setting eq.(11) and (15) equal, the propellant surface temperature can be calculated iteratively based on the magnetosonic and sonic conditions. The surface temperature can then be used as boundary condition to solve the heat equation and find the temperature distribution in the propellant slab.

### Optimization

The following model aims to quantify the late time mass losses by including two different effects: (i) the existence of a portion of propellant already evaporated, but, at the moment of current termination, still inside the thruster and (ii) late-time evaporation between two pulses due to the elevated temperature of the propellant slab. While the first depends on the thruster geometry and the plasma density in the moment of discharge termination, the mechanism of the second can be explained quantitatively as follows: Assuming an ideal square wave discharge current, then according to the idealized model (eq.(11)), the required mass to sustain the discharge varies linearly with time. The depth of the heat flux from the plasma into the propellant scales as the square root of time (see fig. 1). These two statements are equivalent to the two curves depicted in fig. 2. Hereby is  $d_{EV/DC}$  the thickness of the layer which is elevated above decomposition-/evaporization- temperature and  $d_{EM}$  the equivalent to the amount of mass required by the discharge. At a certain time, in the following called the optimum pulse time  $t_{opt}$

, these two curves intersect with each other. If the current pulse ends before reaching this optimum pulse time, the temperature of a certain amount of propellant is elevated above evaporation/decomposition temperature. This part of gaseous propellant will thus exhaust at low thermal velocities and therefore minimally contribute to the impulse bit, thus degrading thruster efficiency. To utilize the propellant more efficient the current pulse has to be adapted in magnitude and in duration to the material properties of the propellant.

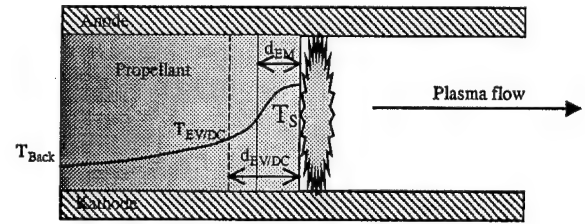


Fig.1: Schematic of a PPT with the two depths  $d_{EV/DC}$  and  $d_{EM}$ , the surface temperature  $T_s$  and evaporation/decomposition temperature  $T_{EV/DC}$

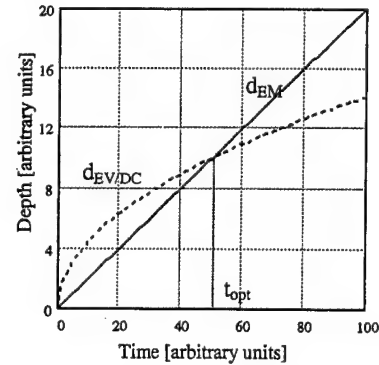


Fig.2: Required depths to sustain the discharge and mass elevated above vaporization temperature

Based on the idealized model described above a simple numerical code was developed to solve eq.(15) for the surface temperature. Based on this temperature the temperature distribution in the propellant slab was evaluated and the optimum pulse times were calculated<sup>2</sup>.

Using the optimum pulse times calculated hereby as a starting points, the full blown magnetohydrodynamic code MACH2 was

used in order to verify the idealized model and eventually refine the results. The results of this comparison are presented in the next chapter.

#### Analytic and numeric results

The idealized model and the pulse optimization procedure were invoked for four different kinds of propellants: Teflon<sup>®</sup>, water, lithium, and cesium. Including

Teflon<sup>®</sup> allows comparisons of the traditional propellant Teflon<sup>®</sup> with other potentially advantageous alternatives. Water is especially interesting in combination with In-Situ-Propellant-Production [4], lithium and cesium can offer a wider envelope of the feasible Thrust-to-Power ratio due to their special individual material properties. Some material properties are summarized in table 1.

	Mass [amu]	1 <sup>st</sup> ionization energy [eV]	2 <sup>nd</sup> ionization energy [eV]	Thermal diffusivity [m <sup>2</sup> /s]	Heat capacity [J/kgK]	Heat of Vaporization [J/kg]	Density [kg/ m <sup>3</sup> ]
Teflon <sup>®</sup>	100	92.2	280.9	$1.28 \cdot 10^{-7}$	1250	$2.1 \cdot 10^6$	2150
Water	18.02	40.8	75.9	$1.47 \cdot 10^{-7}$	4179	$2.4 \cdot 10^6$	997
Lithium	6.94	5.39	81.0	$4.44 \cdot 10^{-5}$	3600	$2.1 \cdot 10^7$	530
Cesium	132.9	3.89	27.1	$8.0 \cdot 10^{-5}$	240	$5.1 \cdot 10^5$	1870

Tab.1: Material properties for the investigated propellants

Refinement of the idealized model by use of the MACH2 code allows to include several features which could not be treated as sophisticated in the idealized model. While the results of the idealized model are based on a defined degree of ionization, MACH2 provides through its extensive SESAME library of thermodynamic properties the possibility to calculate the real degree of ionization. Additionally, MACH2 also offers the possibility to define and fix the degree of ionization. In the following, both options – ideal gas assumption with fixed degree of ionization and real equation of state (EOS) models – were used. Only the results of MACH2 gained with fixed ionization degrees allow a direct comparison with the results of the idealized model. The rigorous optimization procedure however, invoked the complete MACH2 capabilities with real EOS models.

A further important difference was the after-pulse treatment. While MACH2 is able to treat the clearing out of the plasma after the termination of the discharge realistically, in the idealized model it was assumed that the plasma leaves the thruster in a finite time (around 1μs) and the heat flux into the propellant slab decays linearly to zero in the same time.

#### Teflon

Initial comparisons with the MACH2 results and the predictions of the idealized model were already discussed<sup>1</sup>. These findings could be confirmed for a broader range of discharge currents (10-40 kA). The values for the mass flow rate in table 2 are for a discharge current of 30 kA.

	$\dot{m}$ [kg/s]		$u^*$ [km/s]	
	Mach2	IM	Mach2	IM
Teflon <sup>®</sup> (Z=1)	--	0.019	--	19.6
Teflon <sup>®</sup> (Z=2)	--	0.011	--	34.1
Teflon <sup>®</sup> (Z=2.1)	0.0115	--	31.5	--
H <sub>2</sub> O (Z=1)	0.0118	0.012	29.3	30.6
H <sub>2</sub> O (Z=2)	0.0094	0.009	40.2	41.8
H <sub>2</sub> O (Z=1.6)	0.0174	--	22.3	--
Li (Z=1)	0.0067	0.021	52.8	18.0
Li (Z=2)	0.0052	0.0052	70.0	69.6
Li (Z=2.15)	0.0031	--	120.8	--
Cs (Z=1)	0.128	0.43	12.0	3.5
Cs (Z=2)	0.127	0.589	13.0	9.2

Table 2: Comparison between the idealized model (IM) and MACH2 results

#### Water

Using water as a propellant for PPT might open many opportunities in the future. Water seems to be abundant on comets, Jupiter's moon Europa and even on asteroids. The availability of essentially

unlimited, extraterrestrial amounts of propellant enables missions which have been impossible to accomplish before due to their high  $\Delta v$  requirements<sup>5</sup>. Therefore, it is important to have a good understanding how PPTs might work with water as propellant. The numerical calculations for both, singly and doubly ionized water showed good agreement with the predictions of the IM. This changed significantly when the ideal gas assumption was replaced by the SESAME data tables. Since the average degree of ionization in a location around the magnetosonic point for a 20 kA discharge is 1.6, a value between the predicted 0.012 kg/s for  $Z = 1$  and the 0.009 kg/s for  $Z = 2$  (see table 2) was expected. However a mass flow rate of 0.0174 kg/s was calculated. The reason for this was found is the failing of one basic assumption in the derivation of the idealized model. For evaluating the mass flow rate it was assumed that the enthalpy change between the stagnation and the magnetosonic point consists mainly of the specific ionization energy (see eq.(8)). This assumption, though true in the case of Teflon<sup>®</sup> fails in the case of water with EOS (see table 3, H<sub>2</sub>O with  $Z=1.6$ ). The  $c_p T$ -term which was neglected at this place in the derivation (see eq.(8) - eq.(11)) is in some cases higher than the specific ionization energy. In general it was found that the overall idealized model scaling with Alfvén critical velocity is valid as long as the specific ionization energy  $\epsilon_i \sim c_p T$  or better,  $\epsilon_i > c_p T$  (see table 2 and 3).

Material	$\epsilon_i / (c_p T)$
Teflon <sup>®</sup> , $Z \approx 2.1$	$> 1.69$
H <sub>2</sub> O, $Z = 1$	1.05
H <sub>2</sub> O, $Z = 2$	1.26
H <sub>2</sub> O, $Z \approx 1.6$	$< 0.66$
Li, $Z = 1$	0.17
Li, $Z = 2$	1.52
Li, $Z \approx 2.15$	$> 1.42$
Cs, $Z = 1$	0.09
Cs, $Z = 2$	0.51

Table 3: Ratios of specific ionization energy to the thermal static specific enthalpy,  $c_p T$ , at the magnetosonic point

### Lithium

Lithium is an alkali earth metal. It requires special precautions in handling but might offset this disadvantage by its high specific second ionization energy  $\epsilon_i$  resulting in a very high specific impulse. The high thermal diffusivity and the very low equilibrium pressure curve – relative to Teflon<sup>®</sup> – caused numerical difficulties. It was necessary to start with an initial temperature distribution above the evaporation temperature in a small layer of the propellant (about 2% of the total layer). Without such an artificial initial temperature layer, operation resulted in a discharge travelling away from the surface (slug-mode) due to the lag of ablating material. However, the influence on steady state conditions is assumed negligible since the chosen initial temperature drops already after around 0.5  $\mu s$  well below the vaporization temperature. Still, the achieved densities of ablated material during a run were in general low. This results in a relative high temperature plasma with relative high ionization degrees around the magnetosonic point of at least 2.1 over a broad range of discharge currents (20 – 70 kA). MACH2 results imply that ablation-fed lithium PPTs will always operate with doubly ionized propellant in this regime of energy levels. However, to investigate the prediction of the IM, MACH2 runs were conducted with fixed ionization degree of one and two. For a ionization degree of two, acceptable agreements between analytic and numerical results were found. The numerical results in terms of mass flow rate and power consumption are slightly lower than predicted by the analytics. In general, the higher the discharge current, the higher the deviations from the predictions. For a discharge current of 30 kA the deviations are around -1%, for 70 kA around -16%. Even higher deviations were found in the case of singly ionized lithium. This is true because of the same reason as in the case with water. The  $c_p T$ - term is getting close to, or even higher than the specific ionization energy, which hurts the assumption that the specific ionization energy dominates the change in flow enthalpy.

Letting MACH2 calculate the degree of ionization instead of fixing it, resulted in general in a degree of ionization slightly above 2 at the magnetosonic point. In the 30 kA case, (see table 2), the ionization degree was 2.15. At this conditions the specific ionization energy was higher than the  $c_p T$  term and the assumption of specific ionization energy dominating the enthalpy change in the flow is valid.

Since the degree of ionization is not exactly one or two, a direct comparison with the idealized model is not possible anymore. However, a qualitative judgement of the results is possible. According to the idealized model a higher degree of ionization results in a lower mass flow rate and higher magnetosonic velocities. MACH2 confirms these trends. A summary of some results is given in table 2 and 3.

#### Cesium

Cesium is like lithium an alkali earth metal. Due to his low ionization energies and high atomic mass it already was used as propellant for ion engines. Due to its high atomic mass it provides the highest Thrust-to-Power ratios of all the here discussed propellants. Cesium is not included in the SESAME tables. Therefore, only idealgas simulations with fixed degree of ionization of one and two were conducted at discharge currents of 60 kA. Lower discharge currents lead to unreasonably expensive computations due to very low time steps. This was even the case when imposing an initial temperature distribution with a temperature above the evaporation temperature like it was done in the case of lithium. The very high thermal diffusivity (about twice the one for lithium and two magnitudes higher than the one for Teflon and water) was identified as reason for this behavior. The heat flux delivered by the discharge is transported away so fast, that not sufficient mass could be ablated. This led as in the case of lithium, to a discharge travelling away from the propellant surface, which, of course, further decreases the amount of, ablated mass.

The results of the MACH2 simulations showed neither for singly ionized nor for doubly ionized cesium good agreements with the predictions of the idealized model. In case of singly ionized cesium, the mass flow rates were more than 300% lower and the power consumption nearly 400% higher than predicted by the analytics. Better agreements were gained for doubly ionized cesium. However, the mass flow rate calculated by MACH2 was still about 30% lower and a power consumption about 50% higher than predicted. It was found that the reason for these bad agreements is the same as in the case of water and lithium. The specific ionization energy is not anymore the main enthalpy change between the stagnation and the magnetosonic condition. Instead deposition of energy to the thermal internal modes dominates (see table 3).

#### **Discussion of the optimization procedure**

Optimization of the mass efficiency reduces the amount of mass, which is expelled after the termination of the discharge. This mass is not electromagnetically accelerated and leaves the thruster with low thermal velocities. Quantitatively one can express the mass efficiency  $\eta_m$  by

$$\eta_m = \frac{1}{1 + \frac{m_{after}}{m_{pulse}}} \quad (17)$$

MACH2 calculations with fixed ionization degrees and EOS were used to investigate the validity of the predictions of the idealized model. For optimization issues, one has to invoke the real equation of state and the ability of MACH2 to calculate the degree of ionization based on temperature and density distributions. Like already mentioned above, in this case one generally does not get an ionization degree of one or two like it was assumed in the idealized model but something different. Therefore, the optimum pulse time, like given by the idealized model, will not be the optimum pulse time for the real case. However, since the mass flow rates increase with decreasing degree of ionization and vice versa, one can

use the optimum pulse times for singly and doubly ionized propellant as a starting point. This was done for all of the propellants and the results are summarized in fig. 3-5.

It was found that Lithium is a special case. In general, both, higher degrees of ionization and lower discharge currents result in larger optimum times. For doubly ionized lithium and a discharge current of 70 kA, an optimum pulse time of about 500  $\mu$ s was calculated<sup>2</sup> according to model presented above in order to get mass efficiencies of about 0.989. MACH2 simulations with 30 kA discharge current – resulting in an ionization degree of about 2.15 – gave already a mass efficiency of 0.99. This mass ratio does not vary for a broad range of discharge currents and is therefore not included in the figures below.

All three figures show the mass flow rate during steady state (plateau) and the mass flow rate after the termination of the discharge due to the processes discussed above. Every figure includes a run for the optimum time  $t_{opt}$  given by the idealized model and additional runs with pulse times deviating from  $t_{opt}$  (deviation from  $t_{opt}$  is given in percentages). On the upper right corner of each figure the dependency of the mass ratio on the deviation (in percentage) from  $t_{opt}$  is depicted.

The idealized model gives for doubly ionized cesium an optimum pulse time of about 400  $\mu$ s. Since already lower pulse times lead to satisfying mass ratios only runs up to 200  $\mu$ s plus a certain time after the termination of the discharge have been conducted.

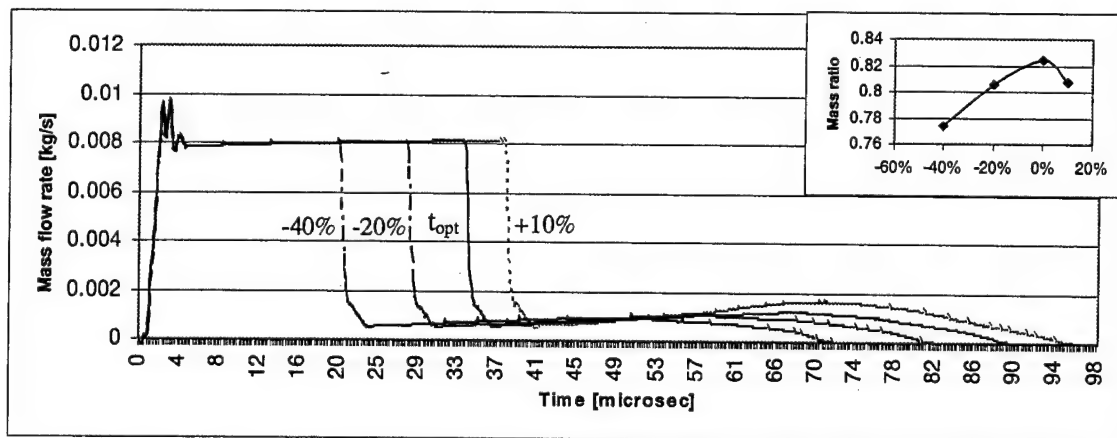


Fig.3: Water mass flow rates and mass ratios for optimum and non-optimum pulse time ( $t_{opt}=8.4\mu$ s,  $Z=2$ , 30kA)

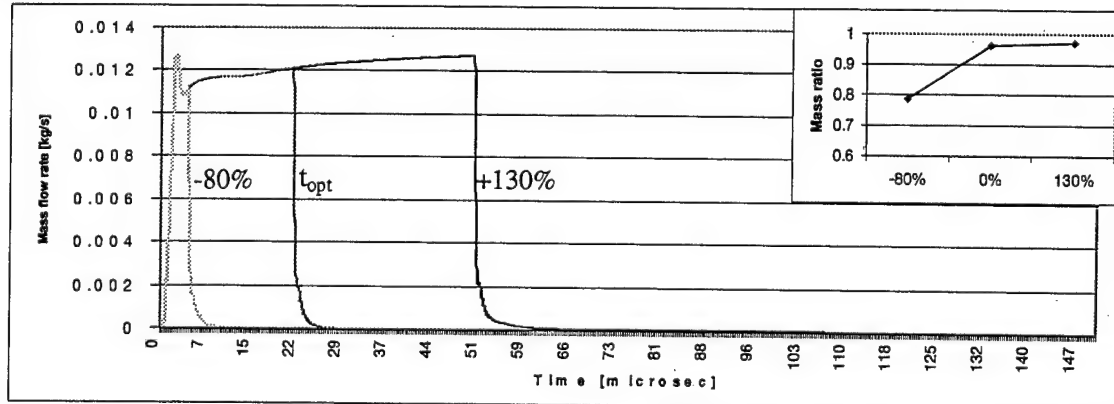


Fig.4: Teflon mass flow rates and mass ratios for optimum and non-optimum pulse time ( $t_{opt}=20.1\mu$ s,  $Z=2$ , 30 kA).

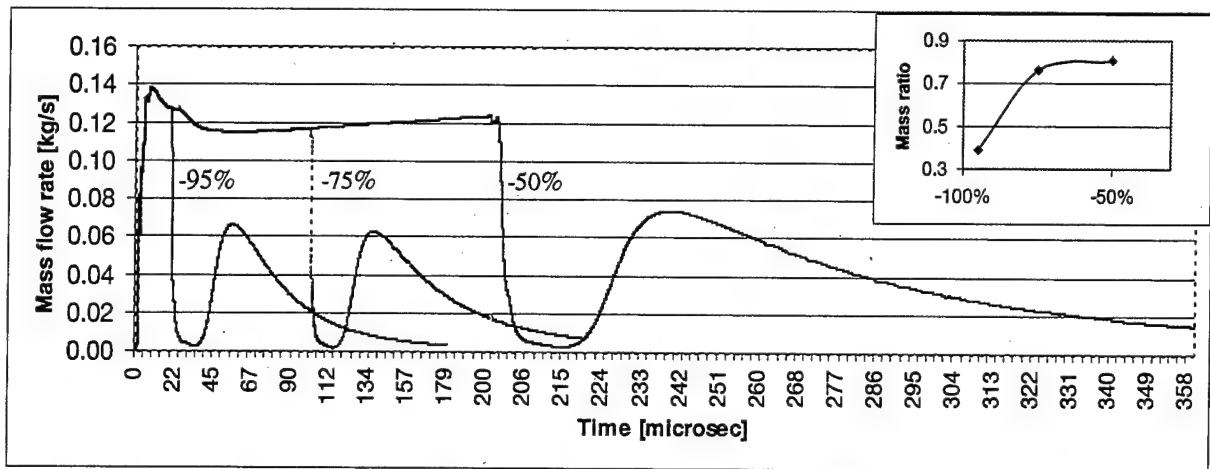


Fig.5: Cesium mass flow rates and mass ratios for non-optimum pulse time ( $t_{opt}=408\mu s$ ,  $Z=2$ , 60 kA).

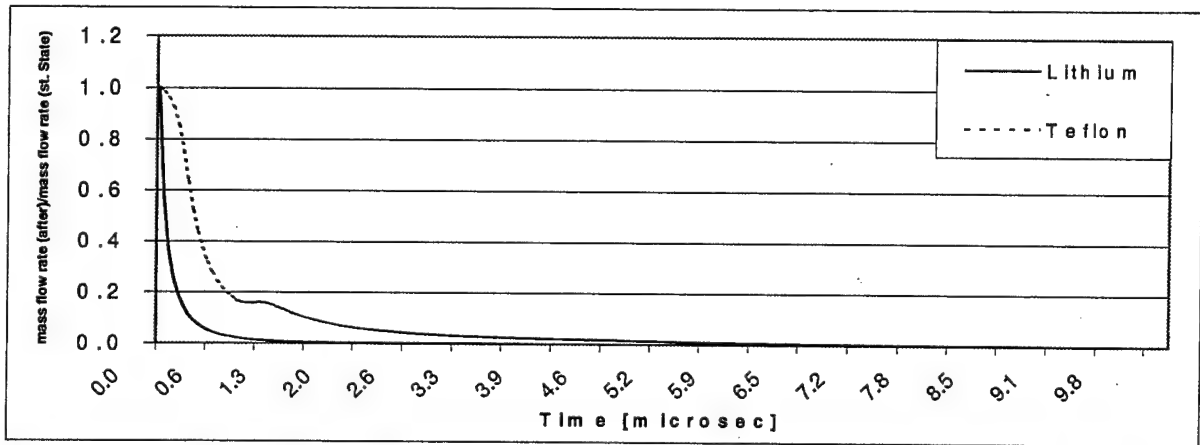


Fig.6: Mass flow rate of Teflon and lithium after the termination of the discharge relative to the steady state mass flow rate

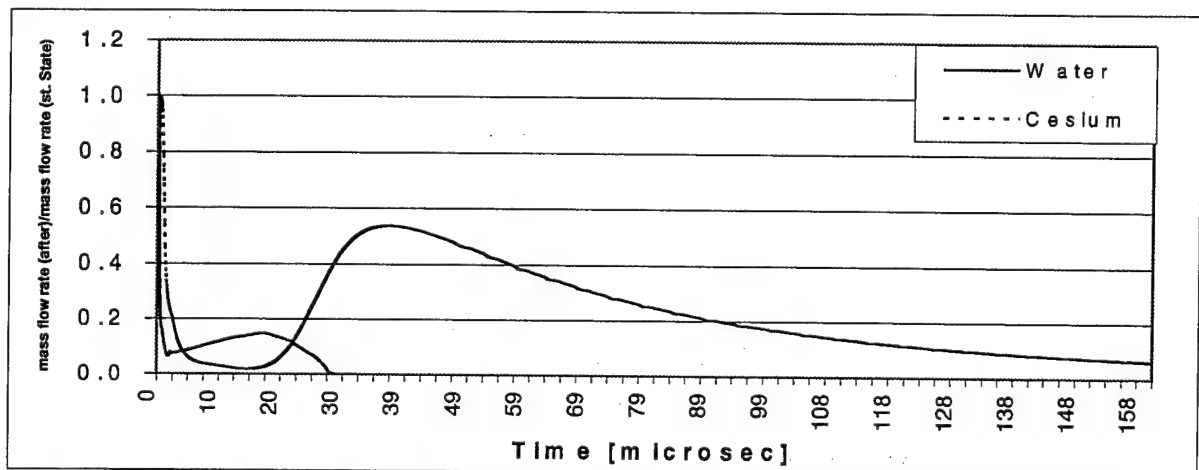


Fig.7: Mass flow rate of water and cesium after the termination of the discharge relative to the steady state mass flow rate

Figure 6 and 7 show the mass flow rate after the termination of the discharge current. It

can be clearly seen that the mass flow rate for water and especially for cesium after the termination of the discharge are substantial.



In the case of cesium mass flow rate after pulse termination reaches about 50% of the mass flow rate during the pulse. Whereas Teflon and lithium rapidly reach very small mass flow rate after the discharge is terminated. Reasons for that might be a combination of material properties with the equilibrium vapor pressure, which is for Teflon® and lithium in the temperature range of interest much lower than for water and cesium.

### Improved mission capabilities

The idealized model predicts a broad range of feasible Thrust-to-Power ratios for the four different investigated propellants (see fig.8).

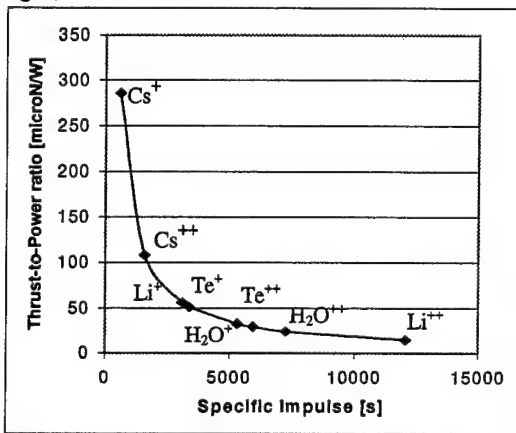


Fig.8: Thrust-to-Power ratio vs specific Impulse

Since it was found that for some of the propellants one major assumption becomes invalid the numbers in fig.8 change in a way that higher velocities at the magnetosonic point were calculated and thus higher specific Impulse and Thrust-to-Power ratios than predicted by the idealized model (see fig.9). However, fig.9 shows also the impressive potential increase in Thrust-to-Power ratios for water and cesium compared to the traditional utilized Teflon®. In general, the increase in range of Thrust-to-Power ratios vs. the specific impulse allows to apply PPT technology for a much broader mission spectrum.

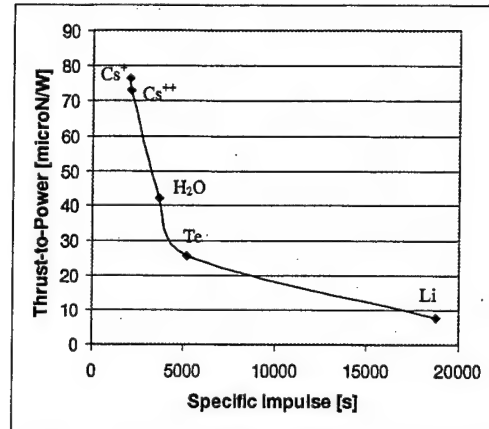


Fig.9: Thrust-to-Power ratio due to the numerical results

### Conclusion

An idealized model for the ablation and acceleration processes in pulsed plasma thrusters was developed to offer optimization guidance and propose directions for improved mission applicability. To verify the model and refine the results the state-of-the-art MHD code, MACH2 was invoked. The calculations were performed for four different candidate propellants: Teflon®, water, lithium and cesium. The analytic model agrees well with the numerical results for Teflon® and for doubly ionized lithium. For water and cesium the assumption that the specific ionization energy is the dominant energy change in the flow seems to be invalid. The velocity at the magnetosonic point does not purely scale with Alfvén critical speed – as proposed by the model – but also includes a thermal contribution resulting in higher velocities at the magnetosonic point, higher specific Impulse and thus generally lower Thrust-to-Power ratios than predicted by the idealized model. However, it was shown that utilization of propellants other than the traditional Teflon® could still offer substantial increase in Thrust-to-Power ratio.

### References

- [1] I.G. Mikellides, P.J. Turchi, Optimization of Pulsed Plasma Thruster in Rectangular and Coaxial Geometries, IEPC 99-211

- [2] R. Corey, Numerical Analysis of the Effect of Propellant Material Properties on Pulsed Plasma Thruster Performance, Thesis, Ohio State University, 1999
- [3] P.G. Mikellides, P.J. Turchi, Modelling of Late-Time Ablation in Pulsed Plasma Thrusters, AIAA 96-2733, July 1996
- [4] P.G. Mikellides, P.J. Turchi, R.J. Leiweke, C.S. Schmahl, I.G. Mikellides,

Theoretical Studies of a Pulsed Plasma Microthruster, IEPC 97-037

- [5] P.J. Turchi, C.A. Scharlemann, Very Long Range Exploration By Means of Electric Propulsion and Cometary Resource Utilization, IEPC-99-189





AIAA-2002-4270

## **Alternative Propellants for Pulsed Plasma Thruster**

C.A. Scharlemann, T.M. York  
The Ohio State University  
Columbus, Ohio

P.J. Turchi  
Air Force Research Laboratory  
AFRL/DE, Kirtland AFB, NM

38<sup>th</sup> AIAA/ASME/SAE/ASEE Joint Propulsion Conference  
7- 10 July 2002  
Indianapolis, Indiana

For permission to copy or to republish, contact the copyright owner named on the first page.  
For AIAA-held copyright, write to AIAA Permissions Department,  
1801 Alexander Bell Drive, Suite 500, Reston, VA, 20191-4344.

# ALTERNATIVE PROPELLANTS FOR PULSED PLASMA THRUSTERS

**Carsten A. Scharlemann**  
The Ohio State University  
Aero/Astro Laboratory  
2300 West Case  
Columbus, OH 43235  
[scharlemann.1@osu.edu](mailto:scharlemann.1@osu.edu)

**Thomas M. York**  
The Ohio State University  
Aero/Astro Laboratory  
2300 West Case  
Columbus, OH 43235  
[york.2@osu.edu](mailto:york.2@osu.edu)

**Peter J. Turchi**  
Air Force Research Laboratory  
AFRL/DE, Kirtland AFB, NM  
[Peter.turchi@kirtland.af.mil](mailto:Peter.turchi@kirtland.af.mil)

## Abstract

Pulsed Plasma Thrusters (PPT) are well known for their simplicity and low power requirements. There are various mission scenarios, where exactly these qualities could make PPTs preferable to other propulsion technologies. To qualify PPTs for a broader range of mission scenarios, it will first be necessary to increase their range of performance, for example, to increase their thrust to power ratios and specific impulse respectively. It was theoretically shown in the past that the utilization of propellants, other than the traditionally used Teflon<sup>®</sup>, is a promising possibility.

The present paper describes the new PPT vacuum facility, which was designed and built for the purpose to test alternative propellants. Initial experiments with alternative propellants, like water, are presented. Diagnostics to evaluate the performance of the electric circuits and the thruster itself, included Rogowski coils, photometry, and Langmuir probes. Furthermore, pressure probes were used for the evaluation of the performance in terms of impulse bits and thrust. This technique is described and their results are presented.

## Introduction

Since several decades Pulsed Plasma Thrusters (PPT) are not only investigated in research labs but also widely utilized for north-south stabilization on satellites. Even though they are in terms of efficiencies inferior

to other electric propulsion systems, they are well known for their structural simplicity and their low average power consumption. Both of these attributes might qualify them in the future for missions beyond north-south stabilization. Unfortunately their utilization is at this time very limited, not only due to their low efficiency but

also because of their limited thrust to power range.

Many efforts were undertaken to understand and improve the efficiency of PPTs. During a discharge, a certain amount of propellant is being ablated and at the same time dissociated, ionized and then accelerated to high exhaust speeds. Already since the beginning of the PPT research it is well known that the portion of propellant which undergoes this sequence of events is only a small fraction of about 10%<sup>1,2</sup>. This poor mass utilization represents a main contributor to the low efficiency of PPTs. In the recent years several theories tried to explain the disposition of the residual 90%, including the existence of macroparticles coming off the propellant surface during the discharge<sup>3</sup> and late time evaporation due to elevated temperature<sup>4</sup> of the Teflon<sup>®</sup>.

In an effort to understand the extent of the late time evaporation, a program at The Ohio State University was initiated. Postulating that controlling the duration of the discharge one could only ablate as much material as the discharge can accelerate, an analytic model was developed to determine the length of this optimized discharge duration<sup>5</sup>. The so gained optimized discharge time was used as input into the time-dependent 2½ dimensional magnetohydrodynamic code MACH2 to calculate among other things the efficiencies and the resulting thrust to power ratio<sup>4</sup>. This effort was not limited to Teflon<sup>®</sup>, the traditional propellant for PPTs, but included also water, cesium, and lithium. It was shown that indeed the choice of the discharge duration influences the efficiency significantly. The results of this program showed also the impressive improvement in thrust to power range by using propellants other than Teflon<sup>®</sup> (see

Fig.1). These results triggered the interest in an experimental verification of the improvements when alternative propellants are utilized.

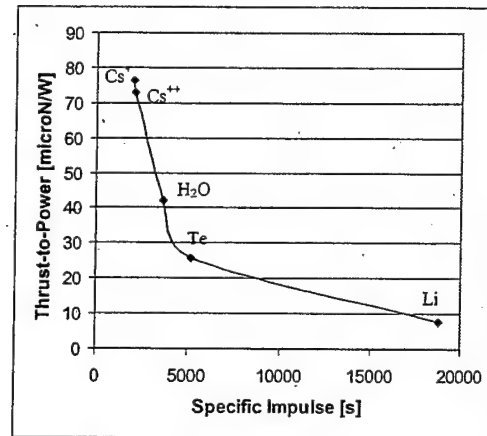


Fig. 1: Variation of thrust to power ratio vs. specific Impulse depending on the choice of propellant (based on MACH2 calculations)

It was decided that in order to do so, water was the propellant of choice. This choice has several reasons. Our initial theoretical predictions show distinguishable differences in thruster performance when water instead of Teflon<sup>®</sup> is utilized. Furthermore, from experimental point of view, water is relatively easy to handle compared to lithium and cesium. Additionally there is increasing interest in water as propellant in the electric propulsion community<sup>6,7,8</sup>. This interest is supposed to grow in the upcoming years in connection with In-Situe-Resource-Utilization<sup>9</sup> and the recent findings that water is far more abundant in space than expected.

### Experimental apparatus

A new vacuum facility was build up at the Ohio State University. The new vacuum facility has several features, which makes it superior compared to the facility utilized before at Ohio State. The compact design of the vacuum system and the utilization of a turbomolecular

pump (NT 220, Leybold-Heraeus) in conjunction with a conventional roughing pump allows base pressures typically around  $4 \times 10^{-6}$  Torr. The convenient small vacuum chamber (Pyrex bell jar, diameter and length of 0.46 m and 0.71 m respectively) and the short vacuum lines reduces the time to reach the minimum pressure to approximately 2 hours, allowing a very efficient and flexible operation. Furthermore the Pyrex vacuum chamber allows optimum visual inspection of the experiment.

The vacuum chamber is located in a plexiglass cage to protect personal and

equipment in case of an imploding chamber. Ventilation ducts at the rear end of the cage are provided to reduce the load on the cage in such a case. The PPT is mounted on a platform inside of the vacuum chamber. This table can be moved several inches up or down and can also be rotated to allow simple handling for the planned spectroscopic diagnostic. Special efforts were undertaken to minimize the danger of electric arcing between the thruster and the structures inside the chamber. All parts inside the vacuum chamber, facing the high voltage parts of the thruster are made of plexiglass.

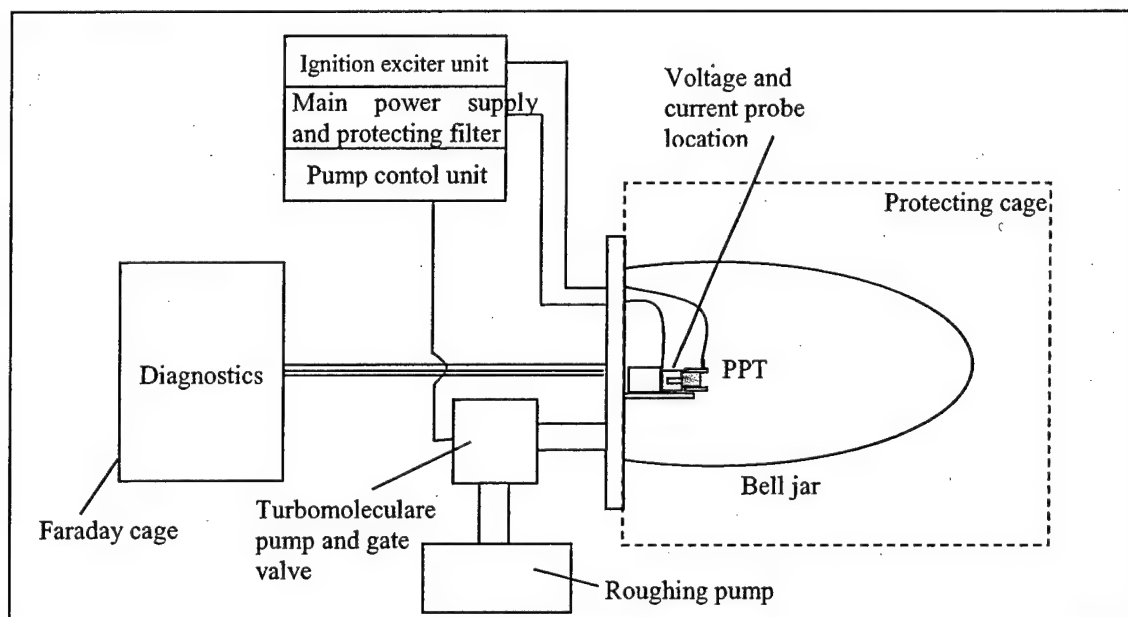


Fig.2: Schematic of the experimental apparatus

### Water feeding mechanism

While the feed mechanism in a standard PPT utilizing Teflon<sup>®</sup> is in general simply a spring pushing the propellant bar against the retaining shoulder in the anode, the problem of feeding a gaseous propellant into a pulsed plasma thruster is more challenging. In the past, this was done by very sophisticated gas feeding system combined with a complicated

triggering systems<sup>10,11</sup>. Even though this results in reportedly high propellant utilization efficiencies it changes an initially very simple system in a highly complex one. In an effort to retain the simplicity of PPTs, a new, extremely simple and robust system was developed. Main objective is hereby not propellant efficiency but experimental simplicity.

The general idea is to utilize the water permeability of Teflon<sup>®</sup> to feed water into the discharge area. The water is stored in a small plenum under atmospheric pressure and is fed to the thruster via a tube. Before it can enter the thruster it has to diffuse through the Teflon<sup>®</sup> bar. The diffusion process is governed by Darcy's law and the mass flow rate can in his simplest form be expressed as:

$$q = \rho \cdot k \cdot A \cdot \frac{dh}{dl}$$

with the density  $\rho$  of water, the coefficient of permeability  $k$ , the cross sectional area  $A$  of the flow and the total head gradient (equivalent to the pressure gradient) over the length of the Teflon<sup>®</sup> bar  $dh/dl$  (see Fig.3).

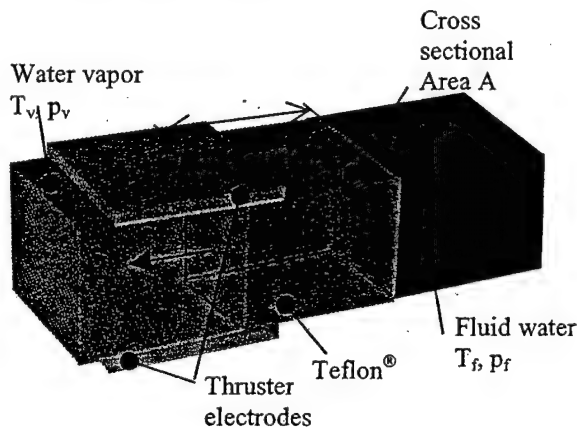


Fig.3: Schematic of the water feed mechanism

A very convenient trait in dealing with such a system is the number of variables one can easily influence: the geometry and size of the contact surface  $A$  between the solid Teflon<sup>®</sup> and the fluid water, the length of the Teflon<sup>®</sup> bar or alternatively the pressure in the propellant plenum, both influencing the pressure gradient. The permeability coefficient can be influenced by the choice of material. For example, Teflon<sup>®</sup> with different densities can be utilized or

layers of different material can be combined in order to increase or decrease the permeability.

For initial experiments the material of choice was a 2.54 cm long Teflon<sup>®</sup> bar. The inside of the water plenum is under atmospheric pressure, resulting in a pressure gradient of roughly 0.4 bar/cm and the contact surface area had a maximum size of 0.32 cm<sup>2</sup>. The side walls of the Teflon<sup>®</sup> bar were covered with a glue to prevent water vapor exiting the Teflon<sup>®</sup> bar on any location beside the wall facing the discharge area.

In a simple experiment, conducted to determine the flow rate, the water feed system was placed in the vacuum chamber. After the vacuum chamber was pumped down, the main gate valve separating the chamber from the pumps was closed and the pressure rise as a function of time was measured. Assuming that only water vapor is responsible for the pressure rise (the pressure rise due to influx (air) in the chamber through walls and sealings is only about one percent of the mass flow rate from the water feed mechanism and was therefore neglected) and assuming further ideal gas conditions the mass flow was determined to be 65 pg/ $\mu$ s. It has to be noted that this is the mass flow rate when the thruster is not operating. During operation it is expected that this mass flow rate changes. This is mainly due to thermal effects and also to a pressure gradient caused by the discharge itself acting in opposite direction of the hydraulic pressure. Determination of the mass flow rate during operation is subject of further experiments.

### Thruster

A new pulsed plasma thruster was designed, especially suited to use both Teflon<sup>®</sup>, and water. The transmission lines between capacitor and electrodes are two coaxial tubes, arranged such that the connection from the capacitor to the anode is inside the connections to the cathode. They are separated by a 1.3 mm thick insulation composed of mylar foil and high voltage tape to guarantee electric insulation (see Fig.4,5,6) The electrodes dimension are similar to the Ohio State bench mark thruster<sup>12</sup>, in particular, the electrodes are 2.54 cm long, 2.54 cm wide and separated by a 2.54 cm gap. In both cases, for Teflon<sup>®</sup> and water, the propellant was fed through the center of the anode connection.

The discharge is triggered by a standard spark plug connected to an ignition exciter unit, both manufactured by Unison Industries. The ignition circuit is powered by a Lambda power supply, model LQ-410. The discharge frequency is controlled by the output voltage of the power supply but was in general chosen to be once per second.

The thruster was designed to be compatible with different capacitor but for the present paper a 10  $\mu$ F capacitor (Maxwell Laboratories Inc.) with a 5 kV rating and a maximum peak current of 25 kA was utilized. A Glassman High Voltage power supply, series EW, 500 W is utilized to charge the capacitor. Discharge voltage was 2kV, resulting in discharge energies of 20 J. Both, thruster and capacitor are located inside the vacuum chamber during experiments while the main power supply and the ignition circuit are located outside the chamber. A frequency filter was placed between the thruster and the main power

supply in order to protect the power supply against damaging back surges. The diagnostic instruments are situated in a Faraday cage located in the vicinity of the vacuum chamber (see Fig.2).

### Diagnostics

#### Current/Voltage

The voltage was measured across the capacitor with a standard Tektronix voltage probe (TEK5100, attenuation factor x100). The discharge current was measured with a Pearson current monitor (model 5046) able to measure peak currents up to 25 kA with an accuracy of +1%, -0% and a wide-band frequency response. Both probes were connected to an oscilloscope. The location of the current and voltage probes can be seen in figure 2.

#### Langmuir probes

Electron temperature and number density can be measured with Langmuir probes. For the present paper we utilized a double Langmuir probe. The probe tips are made of 1.0 cm long and 0.127 mm thick tungsten wire. The separation distance between the two tips is 5 mm. Except the one centimeter long tips, the tungsten wire was insulated with 0.2 cm diameter pyrex tubes fused together with the tungsten wire. The connection to the diagnostics was provided by soldering the tungsten wires to coaxial cables. The outer leads of the coaxial cables are soldered to 0.3 cm diameter brass tubes, which provided the electric shielding. These brass tubes again were housed in 0.5 diameter pyrex tubes and sealed with epoxy.

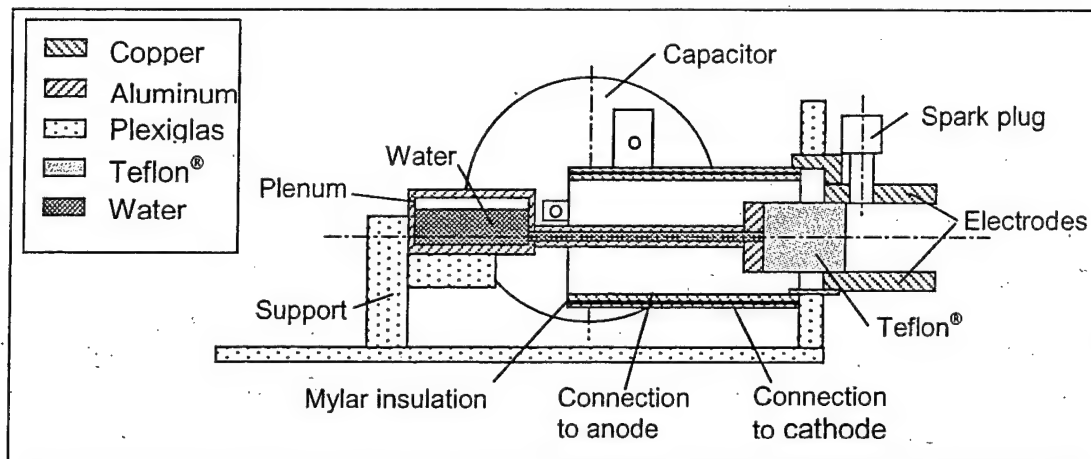


Fig.4: Cross section of the thruster utilizing water as propellant

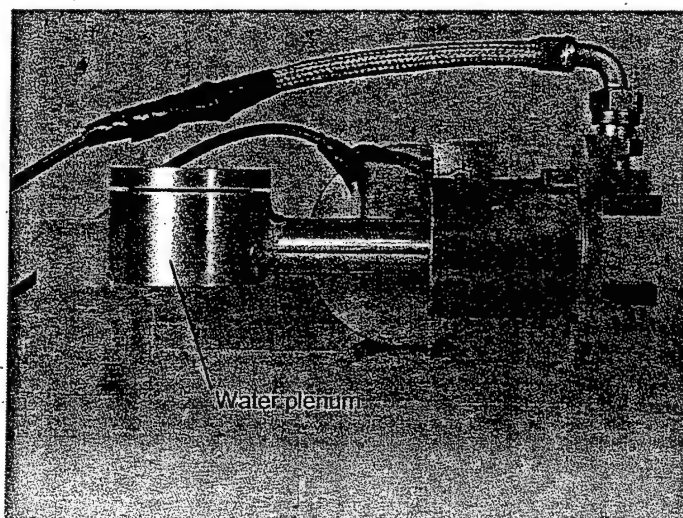


Fig.5: Thruster utilizing water as propellant

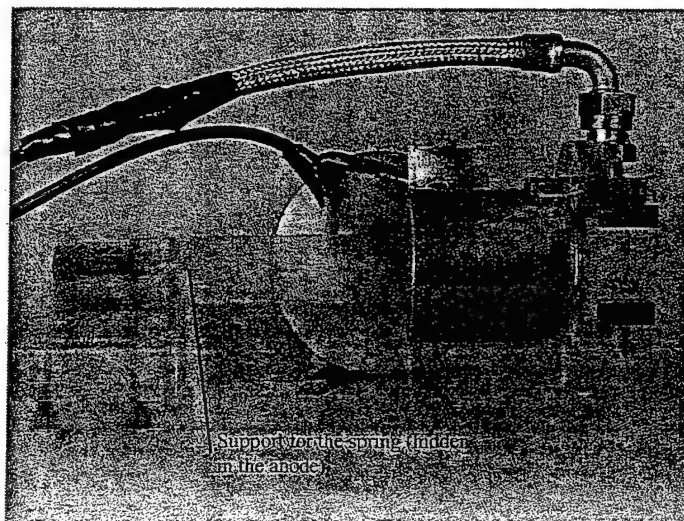


Fig.6: Thruster utilizing Teflon® as propellant



The voltage bias across the probe elements was accomplished by a floating probe circuit similar that used by York and Azevedo<sup>13</sup>. To measure the voltage and current across the probe tips, a Tektronix AC current probe (model P6021), connected to an oscilloscope, and a handheld voltmeter are utilized. After a period of about 10 shots the pressure in the vacuum chamber was allowed to rise to a level where glow cleaning of the probe tips was possible.

#### Pressure probes

Pressure measurements to evaluate thruster performance was utilized in different ways with various techniques already in the past<sup>14,15</sup>. The here presented pressure probe was designed and utilized originally for MPD experiments<sup>16,17</sup>. The probes were designed to withstand the relative extreme conditions of a plasma environment (thermal loads and electromagnetic noise) and have a high frequency response. The core of the pressure probe is a disk of piezoceramic material (PZT-5A) mounted to a backing road with a conducting epoxy (see Fig.7) The disk and the backing road are encased in a conducting shell, separated by a mylar foil around the circumference to prevent electric contact with the piezoceramic disk. The necessary electric contact between the front of the piezoceramic disk and the conducting shell is provided by a thin layer of silver paint. The whole unit is placed in a quartz tube, which has a flat fused end. A coax cable provides the electric contact to the electronic circuitry outside the quartz tube.

The quartz tube provides electric and thermal protection and at the same time

allows stress waves to be transmitted to the piezoceramic disk.

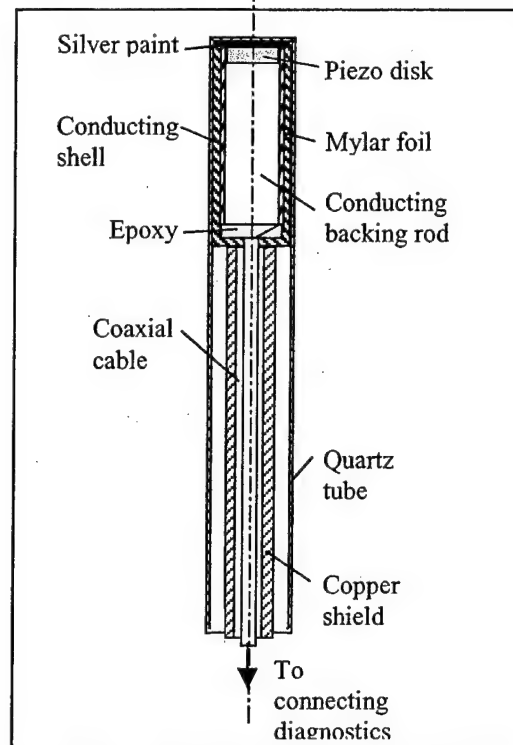


Fig.7: Cross Section of the pressure probe

In the occurrence of pressure, a charge difference built up across the element and is manifested as a voltage transmitted through the connecting coaxial cable to an amplifier and a line follower. The amplifier and the line follower were built to match the output of the probe and allow the charge signal to be transmitted to an oscilloscope as an amplified voltage signal.

The probe in conjunction with the supporting electronic was calibrated in a shock tube. The utilized shock tube consists of two sections, the driver and the driven section. A thin diaphragm separates these two sections. The pressure probe is located on the far end of the driven section, positioned such that its sensing area is flat with the wall. The driven section is under atmospheric pressure while the driver section is filled



with commercial available nitrogen gas at a pressure above atmospheric pressure. At a well known pressure difference between these two sections the diaphragm will burst. As this happens, a shock wave will travel through the driven section and, after hitting the closed end of the wall, will be reflected as a normal shock. Behind this reflected shock the pressure can be accurately calculated using the normal shock relations for an ideal gas. Comparing the measured value with the analytically gained value allows to calculate the calibration constant. The utilized pressure probe has a calibration constant of  $23.8 \text{ (N/m}^2\text{)/mV}$ . The pressure probe response for one of this calibration runs can be seen in the Fig.8.

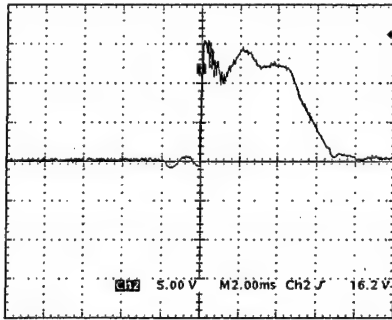


Fig.8: Pressure probe response during the calibration

The impact pressure of a PPT measured by the pressure probe consists of a static and dynamic term and can be written as:

$$p_{\text{impact}} = (n_e + n_i)kT_e + n_i m_i u_{\text{exit}}^2$$

where  $n_e$  and  $n_i$  are the number densities of the electrons and ions respectively,  $T_e$  is the electron temperature,  $m_i$  the ion mass, and  $u_{\text{exit}}$  the exit velocity. By assuming axial flow only, integration of the impact pressure over the plume area will provide the thrust

$$T = \iint p dA = \iint \rho \cdot u_{\text{exit}}^2$$

and will therefore allow to judge the performance of the thruster

## Experimental results

Initial tests with Teflon<sup>®</sup> as propellant were conducted to verify the operation of the new thruster design. Additionally it was intended to build up a data base with Teflon<sup>®</sup> for later comparison with the thruster when using water as propellant. The current measurements showed a very quite shot to shot behavior. Only very small variations can be observed in general. Fig.9 shows three current measurements each taken with a period of about 5 min in between. The curves are overlapping and can nearly not be distinguished. It is believed that one reason for this reliable discharge behavior is the fact that the discharge area is not enclosed by a nozzle, which from experience is frequently the target of sporadic discharges. Even though this reduces the thermal contribution to the thrust, it is a very convenient trait for certain measurements.

Analyzing the current measurements indicates an average circuit inductance of 146 nH and a average circuit resistance of 18 mΩ. In an effort to reduce the inductance, the current monitor was removed. Utilizing the voltage curve to determine the period of the sinusoidal discharge (see fig.10) indicates an average circuit inductance of 79 nH and a lower average circuit resistance. This result can be further improved by replacing the momentarily screwed connections between capacitor and electrodes with welded ones.

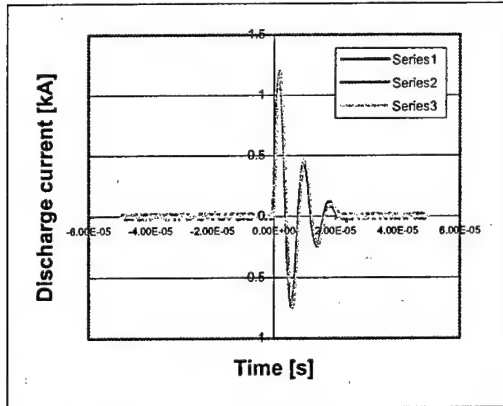


Fig.9: Shot to shot variations in discharge current

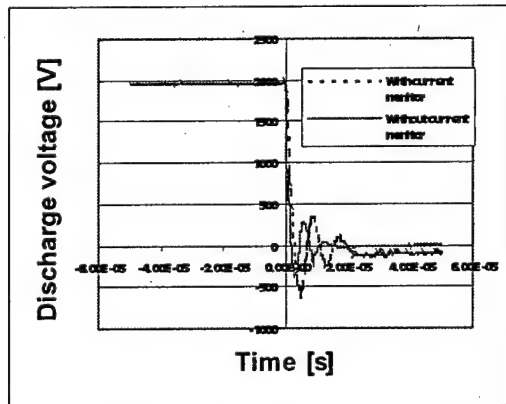


Fig.10: Discharge voltage with and without current monitor

Due to time constraints, initial test of the Langmuir probe diagnostics were done only for the case with Teflon<sup>®</sup> as propellant. In order to determine the exhaust speed of the fast ions the probe was positioned at the exit of thruster and in a distance of 2.54 and 5.08 cm distance respectively. The measurements show an occurrence of two peaks (see Fig.11) of the measured probe current, already observed by other groups<sup>18</sup>.

For each position 10 measurements of the time when the first peak occurred were taken and subsequently averaged. Between the exit and 2.54 cm an average velocity of 45 km/s and between 2.54 cm and 5.08 cm an average velocity of 36 km/s were calculated.

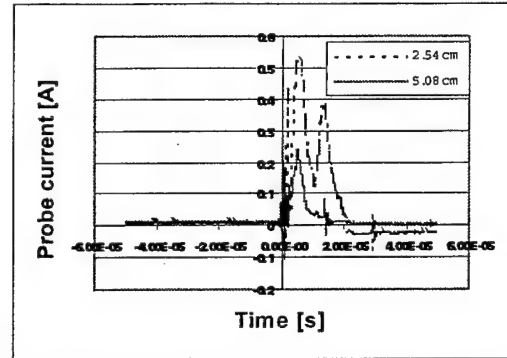


Fig.11: Langmuir probe current at a distance of 2.54 cm and 5.08 cm from thruster exit

Water was successfully fed into the thruster with the above described feeding mechanism at a constant propellant flow rate of 65 pg/μs. Increasing the mass flow to 210 pg/μs by increasing the contact surface  $A$  (see Fig.3) between the fluid water and the Teflon<sup>®</sup> caused occasional sporadic discharges before the capacitor could be charged up to the intended 2 kV or before the spark plug triggered the discharge. This was completely prevented when the mass flow rate was reduced to the above mentioned value of 65pg/μs.

When water is fed through the Teflon<sup>®</sup> into the discharge area, it was observed that after a period of about 5000 shots the for Teflon<sup>®</sup> characteristic visually observable, depression in the middle of the propellant surface is missing. This is believed to indicate that, indeed, the discharge utilizes at least partially the provided water vapor.

In an effort to measure differences in the discharge behavior between water and Teflon<sup>®</sup> the voltage distribution during the discharge was measured. Both cases have about the same shape and period but for the case of water, the peak voltages are slightly smaller (see Fig.12). If this is due to the effect of

utilizing a different propellant will be subject of further research.

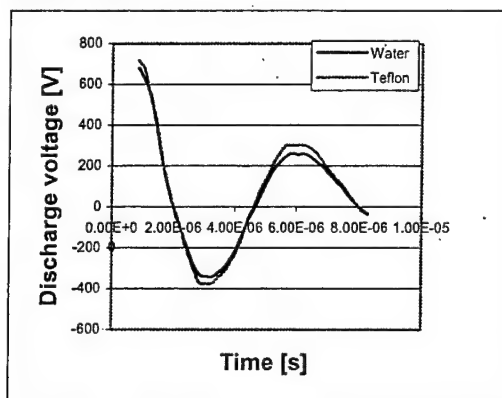


Fig.12: Discharge voltage for water and Teflon<sup>®</sup> operation

### Conclusions

A new pulsed plasma thruster was designed and successfully tested. The thruster is able to utilize either Teflon<sup>®</sup> or a mixture of water and Teflon<sup>®</sup> as propellant. This was implemented by developing a new water feeding system exploiting the water permeability of Teflon<sup>®</sup>. This feeding system is independent of any sophisticated triggering system and therefore conserves the inherent simplicity of pulsed plasma thruster. Water in a constant mass flow of 65 pg/ $\mu$ s was fed into the thruster. Visual inspection of the Teflon surface indicates that the discharge is indeed utilizing the provided water. A small difference in the discharge voltage distribution might support this result.

To verify the results and to identify the performance differences between using Teflon<sup>®</sup> only and a water/Teflon<sup>®</sup> mixture, an array of diagnostic instruments was established, including Current/voltage measurements, Langmuir probes and pressure probes. These diagnostics will be utilized in the future to identify the differences in a PPT utilizing a certain amount of water

as propellant versus a purely on Teflon<sup>®</sup> operating thruster.

### Acknowledgments

The research described in this paper was carried out at The Ohio State University under a contract with AFOSR. Very much appreciated is the help of the following persons: Hani Kamhawi from NASA GRC and Tom Veit from the Aero/Astro Laboratories of The Ohio State University.

### References

- [1] Analysis of Solid Teflon Pulsed Plasma Thruster, R. J. Vondra, K. Thomassen, A. Solbes, Journal of Spacecraft and Rockets, Vol. 7, No. 12, Dec. 1970
- [2] Pulsed Plasma Microthruster Propulsion Systems for Synchronous Orbit Satellite, W.J. Guman, D.M. Nathanson, Journal of Spacecraft and Rockets, Vol. 7, No. 4, Dec. 1970, pp 409-415
- [3] AIAA-96-2723, Investigation of Propellant Inefficiencies in a Pulsed Plasma Thruster, G.G. Spanjers, K.A. McFall, F.S. Gulczinski III, and R. A. Spores, OL-AC Philips Laboratory, JPC, July 1996
- [4] AIAA-99-2301, "Optimization of Pulsed Plasma Thrusters for Microsatellite Propulsion", P.J. Turchi, I.G. Mikellides, P.G. Mikellides, H. Kamhawi, JPC, June, 1999
- [5] AIAA-00-3620, Pulsed Plasma Thruster Variations for Improved Mission Capabilities, C. A. Scharlemann, R. Corey, I.G. Mikellides, P.J. Turchi, P.G. Mikellides, 34<sup>th</sup> JPC, July 2000, Huntsville, Alabama
- [6] IEPC-01-148, Impact of Performance Scaling on Mission Analysis for Gas-Fed Pulsed Plasma Thruster, J.K. Ziemer, R.A. Petr, 27<sup>th</sup> IEPC, Oct. 2001

- [7] IEPC-01-170, Conceptual Design of a Synergistic Propulsion System for the International Space Station (ISS), J. Wilms, A. Hinueber, G. Nentwig, M. Auweter-Kurtz, 27<sup>th</sup> IEPC, Oct. 2001
- [8] IEPC-01-238, "Performance measurements Using a Sub-Micronewton Resolution Thrust Stand", J.K. Ziemer, 27<sup>th</sup> IEPC, Oct., 2001
- [9] IEPC-99-189, "Very Long Range Exploration by Means of Electric Propulsion and Cometary Resource Utilization", P.J. Turchi, C.A. Scharlemann, IEPC, 1999
- [10] AIAA-98-3803, "Effects of Ignition on Discharge Symmetry in Gas-Fed Pulsed Plasma Thrusters" J.K. Ziemer, T.E. Markusic, E.Y. Choueiri, D. Birx, 34<sup>th</sup> JPC, July, 1998
- [11] AIAA-99-2289, "Is the Gas-Fed PPT an Electromagnetic Accelerator? An Investigation using Measured Performance, J.K. Ziemer, E.Y. Choueiri, D. Birx, 35<sup>th</sup> JPC, June, 1998
- [12] AIAA 96-2732, Design and Operation of a Laboratory Bench-Mark PPT, H. Kamhawi, P.J. Turchi, R.J. Leiweke, The Ohio State University, Columbus, Ohio, R. M. Myers, NYMA Inc., Cleveland, Ohio
- [13] Air Force Report, Contract No. FO4611-84-K-0010, "Langmuir Probe diagnostics of Magnetoplasmadynamic Thruster Performance", T.M. York, D.J. Azvedo, Aug., 1984
- [14] AIAA-95-2818, "Pressure Measurements in the Plume of a Low Power Arcjet Nozzle", W.A. Hargus, Jr., M.A. Cappelli, 31<sup>st</sup> JPC, July, 1995
- [15] IEPC-01-152, "Performance Improvement of Pulsed Plasma Thruster for Micro Satellite", M. Igarashi et al., 27<sup>th</sup> IEPC, Oct., 2001
- [16] AIAA 71-196, "Pressure Measurements in the Exhaust Flow of a Pulsed Megawatt MPD Arc Thruster" C.J. Michels, T.M. York, Jan. 1971
- [17] "Stress Dynamics in High Speed Piezoelectric Pressure Probes, T.M. York, Review of Scientific Instruments, Vol.41, No. 4, April 1970, pp 519-521
- [18] AIAA-2000-3258, "Near Field Tribble Langmuir Probe Measurements of a Pulsed Plasma Thruster in a Large Vacuum Facility" L.T. Bryne, E.J. Pencil et al., JPC, 2000

# **28<sup>th</sup> IEPC 2003**

## **IEPC 03-112 INVESTIGATION OF A PPT UTILIZING WATER AS COMPONENT PROPELLANT**

Carsten A. Scharlemann and T.M. York  
The Ohio State University

28<sup>th</sup> International Electric Propulsion Conference  
March 17-21, 2003, Toulouse, France

# INVESTIGATION OF A PPT UTILIZING WATER AS COMPONENT PROPELLANT

**Carsten A. Scharlemann**  
The Ohio State University  
Aero/Astro Laboratory  
2300 West Case  
Columbus, OH 43235  
scharlemann.1@osu.edu

**Thomas M. York**  
The Ohio State University  
Aero/Astro Laboratory  
2300 West Case  
Columbus, OH 43235  
york.2@osu.edu

The utilization of water as propellant in Pulsed Plasma Thrusters has a number of advantages including long time storability, availability and reduced plume contamination. Further impetus for a utilization of water was fueled by computational studies, which were suggesting an improvement of the thrust to power ratio over the standard propellant Teflon<sup>®</sup>.

However, the utilization of water constitutes a major challenge with regard to the fashion it is fed into the thruster. A main objective must be the preservation of the inherent simplicity of Pulsed Plasma Thrusters. As a step towards this goal, a hybrid thruster was developed, which utilizes a mixture of Teflon<sup>®</sup> and water. This paper presents the design of the simple and robust propellant feed system and the experimental investigation of the behavior of a thruster equipped with such a system. Analysis of the discharge current and voltage indicate higher plasma resistance and inductance in the presence of water. Time of flight measurements indicates exhaust velocities twice as high in the case of water compared to standard Teflon<sup>®</sup>. Double Langmuir probe determined the electron temperature and number density to be 3.1 eV and  $4.9 \times 10^{20} \text{ m}^{-3}$  for the water/ Teflon<sup>®</sup> mixture compared to 2.6 eV and  $9.3 \times 10^{20} \text{ m}^{-3}$  for Teflon<sup>®</sup>.

## Introduction

Pulsed Plasma Thrusters are widely utilized due to their low power requirements, simplicity, and reliability. Their main task consists of north-south stabilization of satellites. However, the above listed attributes could also qualify them for future mission like visits to the outer regions of our solar system. But to be part of a future space exploration scenario it will be necessary to improve their performance with regard to their limited specific impulse and their low efficiencies.

One possibility to achieve these goals is the utilization of propellants other than the traditionally used Teflon<sup>®</sup>. Efforts to find a promising alternative to Teflon<sup>®</sup> included LiOH seeded Teflon<sup>®</sup> and different kind of thermoplastics like Halor, Tefzel<sup>1</sup>, variation of the ablative surface properties<sup>2</sup>, and Teflon<sup>®</sup> of different densities, porosities, and level of carbon contains<sup>3</sup>.

Two years ago an effort to utilize water as propellant for PPTs was initiated at the Plasma Dynamic and Propulsion Laboratory of The Ohio State University. The advantages of water are numerous. Numerical simulations have shown a

improvement in thrust-to-power ratio<sup>4</sup>, water is nontoxic, it seems to be abundant in space (e.g. on comets or in the Jovian system etc.), it might reduce plume contamination, and it can be shared with other systems like life support systems or the main propulsion system (for example in case of a NERVA type main propulsion system) - to name only some of the most important advantages.

Main objective of this research was to develop a propellant feed system, which preserves the inherent simplicity of PPTs. The present paper describes the most recent progress in developing such a water feed system and summarizes the diagnostic utilized to investigate and identify performance changes and their results.

### Propellant feed mechanism

One of the main advantages of PPT is their inherent simplicity and in particular the simplicity of the propellant feed system. In a standard ablative PPT (APPT) the feed system consists only of a spring pushing the Teflon<sup>®</sup> bar against a retaining shoulder in the anode, therefore assuring that the ablating surface is always at the same position. Utilizing a non solid propellant like water vapor leads to a variety of challenges. Supplying amounts of water in the  $\mu\text{g}$  range instantaneously into the discharge area such that the whole amount is available when the discharge is initiated can not be solved with any mechanical valve in a straight forward fashion. Methods to inject gaseous propellants combined with a sophisticated system of burst of discharges have been developed and successfully tested<sup>5,6</sup>. However, the complexity of an initially simple system has increased significantly. In an effort to prove the feasibility of water utilization in PPTs and at the same time to preserve their inherent simplicity as much as possible, an alternative propellant feed system was developed at The Ohio State University.

Instead of controlling the mass bit fed into the thruster with a valve, this new concept exploits the water permeability of a porous medium to feed water into the discharge area. The water is stored in a small plenum

under atmospheric pressure and is pushed through the porous medium into the thruster. The mass flow rate  $\dot{m}$  for such a system can be approximated by Darcy's law:

$$\dot{m} = \rho \cdot k \cdot A \cdot \frac{dp}{dl} \quad (1)$$

with the density  $\rho$  ( $\text{kg/m}^3$ ) of water, the coefficient of permeability  $k$  ( $\text{ms/kg}$ ), the cross sectional area  $A$  ( $\text{m}^2$ ) of the flow and the pressure gradient over the length of the diffusion head  $dp/dl$  ( $\text{N/m}^3\text{m}$ ) (see fig.1).

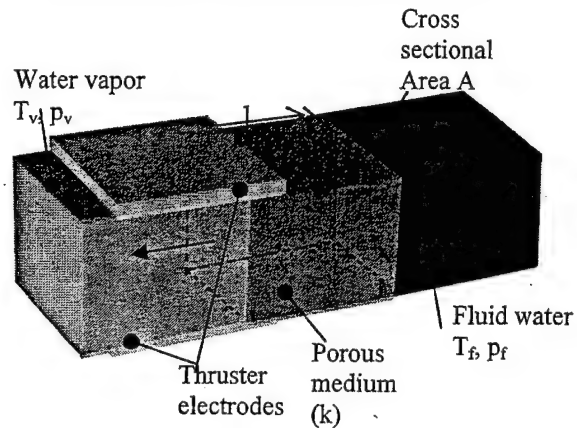


Fig.1: Schematic of the water feed mechanism

A very favorable trait in dealing with this system is the number of easily adjustable variables: the geometry and size of the contact surface  $A$  between the porous medium and the fluid water, the length of the porous medium or alternatively the pressure in the propellant plenum, both influencing the pressure gradient. The permeability coefficient  $k$  can be influenced by the choice of the medium.

The porous medium is connected to a water plenum via an adapter. Several materials and geometries were experimentally investigated and compared to the performance of a regular (dry) Teflon<sup>®</sup> bar. Three of the most important investigated configuration are the following: Teflon<sup>®</sup> (a), Ceramic (b), and a combination of both (c). These 3 configurations are depicted in fig.2. The letter D denotes the surface facing the discharge.



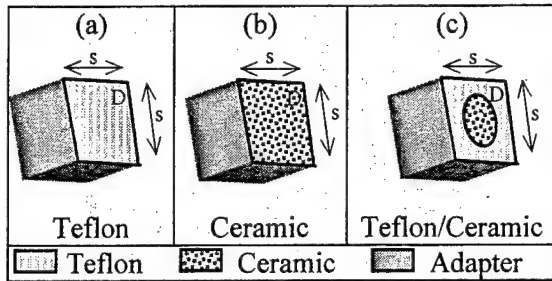


Fig.2: Material and geometry of the different types of porous media ( $s = 2.54$  cm)

Though initial tests with configuration (a) confirmed that water is diffusing through the Teflon® and is being utilized by the discharge, it was later found that the mass flow rate of water through the Teflon® is not sufficient to reduce the ablation rate of Teflon® in a significant way. In an effort to increase the mass flow rate, different porous materials were investigated. Guided by the results of the mass flow experiment described below, a material with higher porosity was chosen. With a 10% porosity ceramic (RESCOR-960) (configuration (b)) the mass flow rate was increased, up from around  $60 \mu\text{g/s}$  to  $300 - 800 \mu\text{g/s}$  (depending on the length  $l$  and the area  $A$  (see fig.1). Another major effect of this configuration was the unwanted reduction of discharge current of about 30% compared to a standard discharge for the Teflon® mode. Initially it was concluded that the reason for this observation might be the starvation of the discharge even with the increased mass flow rate stated above. Since a further increase of the water mass flow rate was not advisable, the discharge had to be sustained with material from other sources. Configuration (c) is the result of this reasoning and it is basically a combination of configuration (a) and (b). Water diffuses only through the center ceramic cylinder (diameter  $1.75$  cm). The outer part made of Teflon® can be seen as a catalyst for the discharge. In the following only configuration (c) will be discussed except if stated otherwise.

### Mass flow experiment

Darcy's law mentioned above is a 1 dimensional, single phase approximation of what is truly a three dimensional flow, which includes at least two phases of water (fluid and vapor). Since it was felt that better experimental values were needed in order to guide the choice of porous materials and its geometry, a mass flow experiment was designed and built. It's design is such that all the parameters mentioned above ( $A$ ,  $l$ , and  $k$ ) can easily be changed (see fig. 3a). Figure 3b shows how the mass flow experiment is assembled in a feed through of the vacuum chamber facing the vacuum side.

In order to measure the water mass flow rate through the test material, the vacuum chamber was pumped down to about 2-5 mTorr. Subsequently the vacuum chamber was separated from the pumps by closing the main gate valve. The mass flow rate through the porous media was then evaluated by measuring the pressure rise in the vacuum chamber over time,  $dp/dt$ , and utilizing eq. 2 (this equation is in the framework of the ideal gas assumption a good approximation since the leakage rate of the vacuum chamber is only about 1-5% of the calculated water mass flow rates).

$$\dot{m}_{H_2O} = \frac{dp}{dt} \cdot \frac{V_{\text{chamber}}}{R_{H_2O} \cdot T} \quad (2)$$

with the vacuum chamber volume  $V_{\text{chamber}}$  [ $\text{m}^3$ ], the temperature  $T$  ( $293^\circ\text{K}$ ) and the specific gas constant for water ( $461\text{J/kg}^\circ\text{K}$ ). With this experiment a much better understanding of the impact of the different parameter in Darcy's law will be achieved and will consequently allow improvement of the design of the water feed system.

### Experimental apparatus and thruster design

The experimental apparatus utilized for this work has been described in the literature before<sup>7</sup> and only the main features will be mentioned here again.



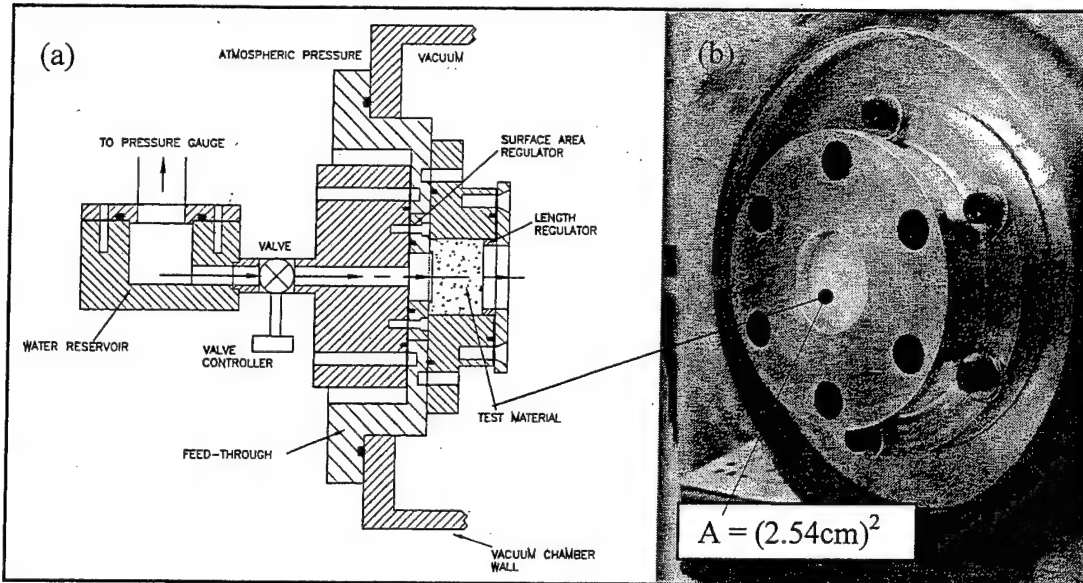


Fig. 3: Cross section (a) and a front view (b) of the mass flow experiment

The vacuum system consists of a roughing pump in conjunction with a turbomolecular pump and allows to reach background pressures of around  $3 \times 10^{-5}$  Torr in a relative short time. However, when operating with water, background pressures of only 3-5 mTorr were achieved due to the constant mass flow rate of water. It is well known that the magnitude of background pressure has great influence on, for example, the discharge behavior and ablation rate. Therefore it was decided to conduct all the experiments at a background pressure between 2-5 mTorr.

A new pulsed plasma thruster was designed and built, especially suited to use both Teflon<sup>®</sup> and water. The transmission lines between capacitor and electrodes are made of a copper annulus, arranged such that the anode annulus is inside the cathode annulus (see fig. 4, 5). They are separated by a 1.3 mm thick insulation composed of mylar foil and high voltage tape to guarantee electrical insulation. This configuration showed a very favorable low inductance, low resistance behavior. The electrodes dimension are similar to The Ohio State University bench mark thruster<sup>8</sup>, in particular, the electrodes are 2.54 cm long, 2.54 cm wide and separated by a 2.54 cm gap. In both cases, the Teflon<sup>®</sup> and water mode, the propellant

was fed through the center of the anode connection.

The discharge is triggered by a standard spark plug connected to an ignition exciter unit, both manufactured by Unison Industries. The ignition circuit is powered by a Lambda power supply, model LQ-410. The discharge frequency is controlled by the output voltage of the power supply but was in general chosen to be about once per second.

The thruster was designed to be compatible with different capacitor but for the present paper a 30  $\mu$ F capacitor (Maxwell Laboratories Inc.) with a 2 kV rating and a maximum peak current of 25 kA was utilized. A Glassman High Voltage power supply, series EW, 500 W is utilized to charge the capacitor. In general the discharge voltage was 1155 V, resulting in discharge energies of 20 J. Both, thruster and capacitor are located inside the vacuum chamber during experiments while the main power supply and the ignition circuit is kept outside the chamber. A frequency filter was placed between the thruster and the main power supply in order to protect the power supply against damaging back surges.

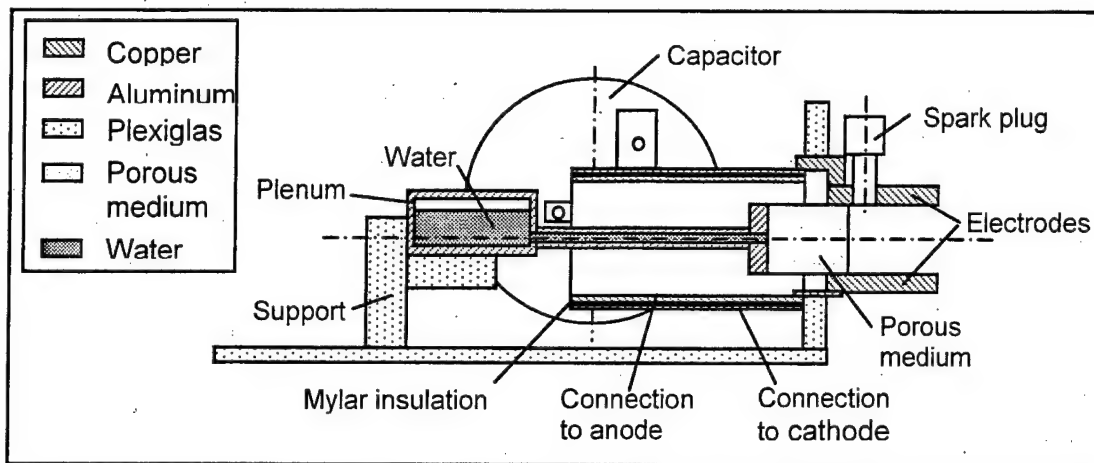


Fig.4: Cross section of the thruster and the water feed system

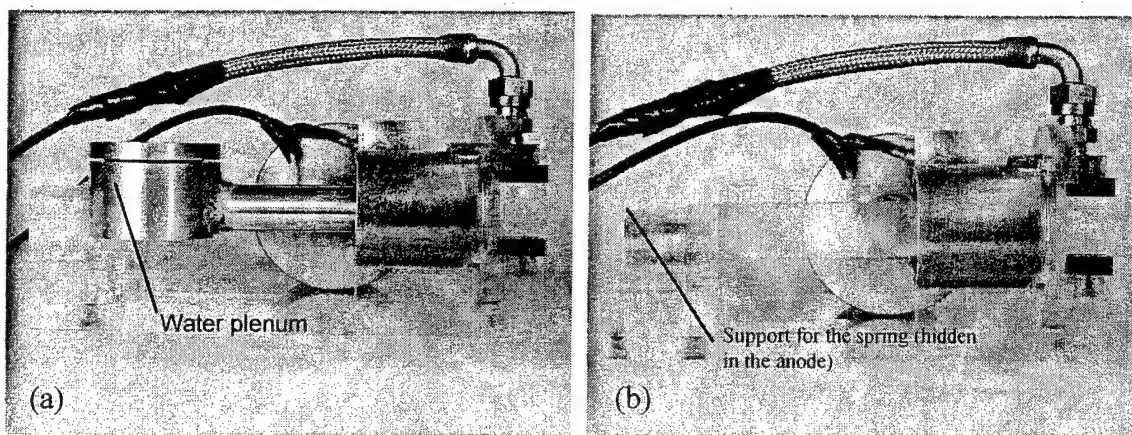


Fig.5: Thruster in the water mode (a) and in the Teflon mode (b)

### Diagnostics

Main objective of the diagnostic was to identify differences between operation in the Teflon<sup>®</sup> and the water mode. For the latter, only configuration (c) (see fig.2) was utilized for the results presented below. As mentioned above, the discharge energy was 20 J for all the experiments.

Double distilled water was utilized for all the experiments to avoid any change of the permeability coefficient due to impurities in the water.

### Mass consumption evaluation

The two different modes of operation, Teflon<sup>®</sup> mode and water mode, require different methods in order to measure the propellant consumption. The mass consumption in the Teflon<sup>®</sup> mode was evaluated by measuring the weight of the

Teflon<sup>®</sup> bar (2.54x2.54x2.54 cm) before and after a run. In order to avoid transition effects<sup>9</sup> and to minimize error due to the weight balance (Mettler AE100) a long time run was conducted. The total run time was nearly 12 hours, split into a 4 hours and a 7 hours period. Every two hours the thruster was switched off for about a minute for a visual check. The discharge frequency was  $1.2 \text{ s}^{-1}$ , resulting in a total amount of discharges of 51,250. Before measuring the Teflon<sup>®</sup> bar after the experiment, it was allowed to adjust to the humidity of the environment for 24 hours. The mass loss per discharge was evaluated to be  $34.8 \text{ } \mu\text{g/discharge}$ .

The evaluation of the amount of water propellant utilized per discharge is not as straight forward. It is assumed that the discharges utilizes material from, at least,

three sources: ablated Teflon<sup>®</sup>, water stored in the capillaries of the porous material, in the following called  $\delta m_s$  and water vapor, which is already between the electrodes at the time of the discharge initiation, denoted in the following with  $\delta m_v$ . While a first approximation for  $\delta m_v$  based on the background pressure in the vacuum chamber is relatively straight forward, this is not the case for  $\delta m_s$ . In order to estimate the magnitude of  $\delta m_s$  the knowledge of several still unknown parameters is necessary. To name only two of the most important, the degree of saturation of the ceramic with water vapor and the thickness of the layer below the ceramic surface which is depleted of water by the discharge.

#### Discharge current and voltage measurements

During thruster operation the discharge current and voltage were monitored. For the latter a standard voltage probe (Tektronix P5100, x100, 2.5kV peak) was utilized to measure the voltage across the capacitor. The discharge current was measured by a house made Rogowsky coil, which was calibrated with a Pearson Current monitor #5046. The Rogowsky coil is attached

around the hot stud of the capacitor and is connected to the oscilloscope via a RC integrator.

In figure 6 the discharge currents between the Teflon<sup>®</sup> and the water mode are compared. In order to reduce errors introduced by shot-to-shot variations each curve is the result of an averaging process including 5 measurements. The third curve in figure 6 represents operation of the thruster with the configuration (c) but with no water supply. This measurement is important to distinguish the differences due to the unique design of the configuration (c) and effects due to the water itself. It is obvious from the comparison that the simple exchange of a Teflon<sup>®</sup> bar with the configuration (c) does not change very much (see table 1). Even though the addition of the ceramic inlay reduces the Teflon<sup>®</sup> surface available for ablation nearly 40%, the discharge seems to find enough material to sustain itself and produces discharge currents only 10% lower than in the case of a standard Teflon<sup>®</sup> case. This changes dramatically when water is supplied. The discharge current peaks are much lower and the time until current reversal is prolonged.

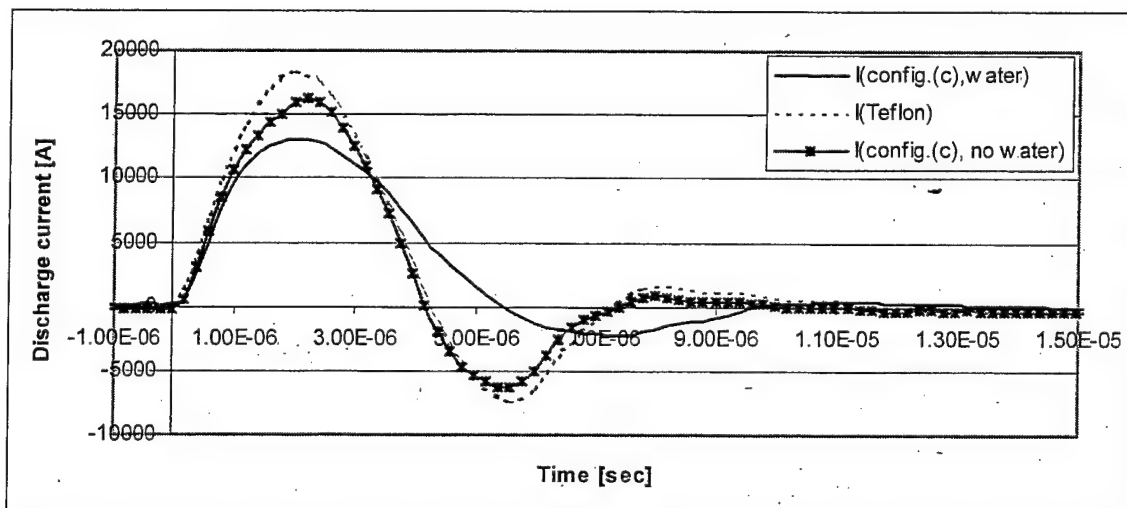


Fig. 6: Examples of the discharge current for standard Teflon<sup>®</sup> and the configuration (c) with and without water

Measuring the discharge curves allows also determination of the circuit parameters. The

circuit consists of the capacitor, the leads from the capacitor to the electrodes and the

plasma discharge itself. Each component has its own resistance and inductance. Since for all three curves above the thruster components like capacitor and leads were the same, a comparison of the overall circuit parameters will give insights into the discharge plasma itself and how it changes when water is introduced.

The total circuit inductance and resistance were calculated with equation 3 and 4 and are summarized in table 1:

$$L = \frac{T^2}{4\pi^2} \cdot \frac{1}{C} \quad (3)$$

$$R = \frac{2 \cdot L}{T} \cdot \ln\left(\frac{I_1}{I_2}\right) \quad (4)$$

with the period  $T$  (sec) of the sinusoidal discharge current, the capacitance  $C$  ( $\mu\text{F}$ ) of the capacitor ( $30\mu\text{F}$ ), the circuit inductance  $L$  (nH), the circuit resistance  $R$  ( $\Omega$ ) and the discharge peak currents  $I_1$  and  $I_2$ .

	Period $T$ [ $\mu\text{s}$ ]	$I_1/I_2$ [kA/kA]	$L$ [nH]	$R$ [m $\Omega$ ]
Teflon	7.3	$18.3/7.3 = 2.5$	45	11.3
Config.(c), no water	6.8	$16.3/6.3 = 2.6$	39	10.9
Config.(c), water	10.4	$13.0/2.23 = 5.8$	91	31

Table 1: Comparison of the circuit parameters

### Langmuir probes

Electron temperature and number density were determined from a semi-graphical analysis of the current voltage characteristic of a double Langmuir probe. The utilized system includes the double Langmuir probe, a supporting floating probe circuit and an oscilloscope (Tektronix, TDS 420A).

The Langmuir probe consists of two probe elements made of 0.127 mm diameter tungsten wire with an exposed surface length of 1 cm. The two tips are separated by a distance of 5 mm. The probe circuit keeps the tips of the probe on a certain voltage potential during a measurement. When the tips get in contact with the plasma ejected by the thruster, a current between the two tips will develop. For a given probe geometry the magnitude of this current is

only a function of the state of the plasma and the applied voltage difference. This current is measured by a Tektronix probe current (P6021), which is connected between the probe circuit and the oscilloscope.

To minimize distortion of the current signal, the probe tips were frequently cleaned through electrical means (glow cleaning). The glow cleaning circuit consists of a high voltage power supply (Keithley Instruments, #246) connected to the probe via a 100 k $\Omega$  resistor to avoid excessive currents in the cleaning circuit. By applying a voltage difference of around 500 V to the tips of the probe a small current between the two tips is generated, which – by means of ion bombardment – then cleans them. The polarity of the probe was switched several times to assure that both tips are evenly clean. For this process it was not required to open the vacuum chamber, however to be effective it was necessary to allow the pressure in the vacuum chamber to rise up to about 300-500 mT.

With the probe geometry as described above and expected values<sup>10</sup> for the electron temperature between 1 to 4 eV and number densities between  $10^{18} - 10^{21} \text{ m}^{-3}$  both requirements for collisionless condition<sup>11</sup> are satisfied ( $r_p \ll \lambda_{ij}, \lambda_{ie}, \lambda_{ee}$  and

$\lambda_{ij}, \lambda_{ee}, \lambda_{ei} > \lambda_D$ ) and the following semi-graphical method to evaluate the electron temperature and density can be utilized. This method requires determination of the current-voltage characteristic of the probe<sup>12</sup> from which the electron temperature  $T_e$  and density  $n_e$  can be computed with the following approximate equations:

$$T_e = \frac{e \cdot I_{sat}}{2 \cdot k} \cdot \frac{dV}{dI} \Big|_{V=0} \quad (5)$$

$$n_e = \frac{I_{sat}}{A_p \cdot e} \left( \frac{k \cdot T_e}{2\pi \cdot m_i} \right)^{-0.5} \quad (6)$$

with the current collecting surface of the probe  $A_p$ , the electron charge  $e$  ( $1.6 \times 10^{-19} \text{ C}$ ), the Boltzmann constant  $k$  ( $1.38 \times 10^{-23} \text{ J/K}$ ), the saturation current  $I_{sat}$ , the average mass of ions  $m_i$ , the electron temperature  $T_e$ .

(°K,  $1\text{eV}=11,000^\circ\text{K}$ ) and the slope of the current-voltage curve  $dV/dI$  for  $V=0$ .  $I_{\text{sat}}$  and  $dV/dI (V=0)_{\text{Teflon}}$  are indicated in fig. 7 for demonstration purpose.

The typical shot-to-shot variations of PPTs are present in the Langmuir probe measurements (even more pronounced in the water mode than in the Teflon® mode). Therefore it was necessary to average several measurements to obtain meaningful results. Two current-voltage characteristics, one for the Teflon® and one for the water mode, are depicted in figure 7. Every point in this figure represents in average 7 measurements taken in a time frame of about 2 minute. Before proceeding to another probe voltage, the pressure in the vacuum chamber was allowed to rise in order to glow clean the probe as described above. Then the chamber was pumped down again and another run was started.

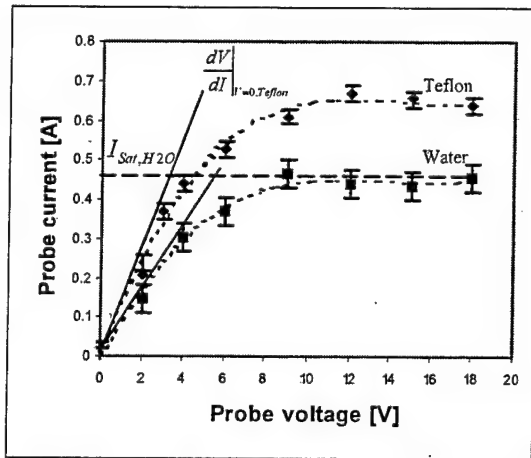


Fig. 7: I-V characteristic for water and Teflon® at a location 7.6 cm downstream of the thruster's exit plane (dashed lines represent third order polynomial fits).

Based on the figure 7 and equation 5 and 6, electron temperatures for the Teflon® and water mode of 2.6 eV and 3.1 eV respectively are calculated.

In order to calculate the number density it is required to estimate the average molecular mass. For the Teflon® mode an average molecular mass of 31 g/mol or molecular mass of  $5.146 \times 10^{-26}$  kg

respectively was assumed<sup>13</sup>. This results in an electron number density of  $9.3 \times 10^{20} \text{ m}^{-3}$ . The exhaust plume in the water mode is composed of the dissociation products of Teflon® and water. As a first approximation for the average atomic/molecular mass in the plume it is assumed that the water-Teflon® ratio in the plasma is equal to the ratio of ceramic surface to Teflon® ablation surface in configuration (c),  $A_c/A_T = 0.4$ . Further assuming that the dissociation products of the Teflon® still have an average molecular mass of  $5.146 \times 10^{-26}$  kg and the water is fully dissociated with an average atomic mass of  $9.9 \times 10^{-27}$  kg, this results in a total average particle mass of  $3.5 \times 10^{-26}$  kg and subsequently in an electron number density of  $4.9 \times 10^{20} \text{ m}^{-3}$  for the water mode.

The Langmuir probe measurements include further important information, the time of arrival (TOF). The time difference between two TOF measurements at two locations downstream of the thruster exit plane allows to determine the thruster exhaust speed. Fig 8 and 9 show the Langmuir probe signal for the Teflon® and the water mode at two different locations, at 7.6 cm (3.0 inches) and 11.4 cm (4.5 inches).

In fig. 8 it can be clearly seen that the probe signal in case of the water mode detects an earlier arrival of the plasma front compared to the Teflon® mode (indicated by the earlier rise of the signal). This time difference increases at a distance further downstream (fig.9), supporting the conclusion that the time lag is due to two plasma fronts moving with different velocities.

The term velocity in this context must be seen as a rather crude term since the plasma exiting the thruster consists of particles with velocities varying over a large range (indicated by the broadening of the peaks). However, in order to allocate an exhaust velocity to the two different modes it was decided to exploit the pronounced first peaks in fig. 8 and 9. Knowing the time difference between the occurrence of a peak at different location allows to calculate an

average plasma velocity. TOF measurements were conducted at 7.6 cm (3.0 in), and 11.4 cm (4.5 in). Based on these measurements velocities of 22.3 km/s

for the water mode and 10.6 km/s for the Teflon<sup>®</sup> mode were calculated.

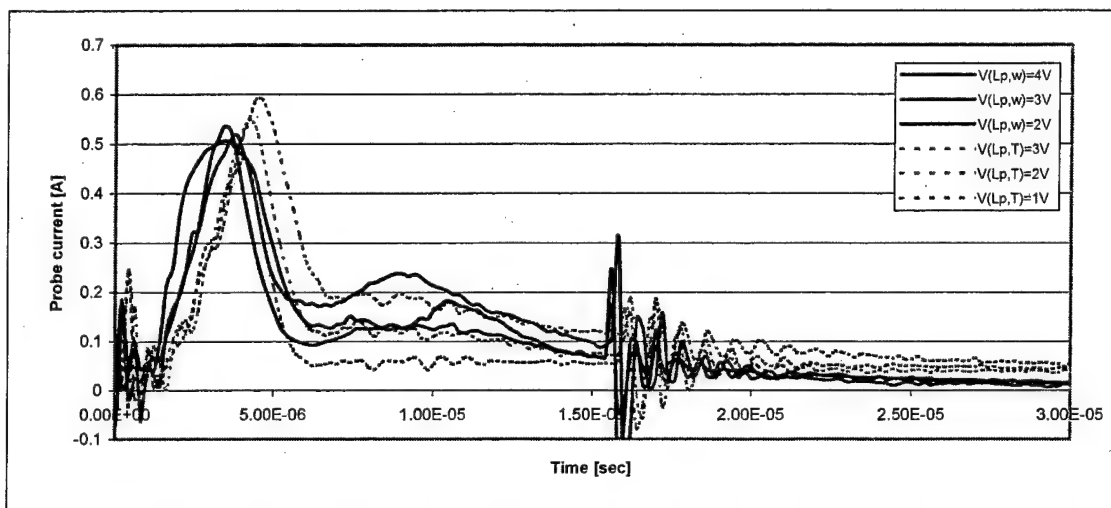


Fig. 8: Langmuir probe current for the Teflon<sup>®</sup> (dashed) and water mode (solid) and for different probe voltages at a location 7.6 cm downstream of the thrusters exit plane

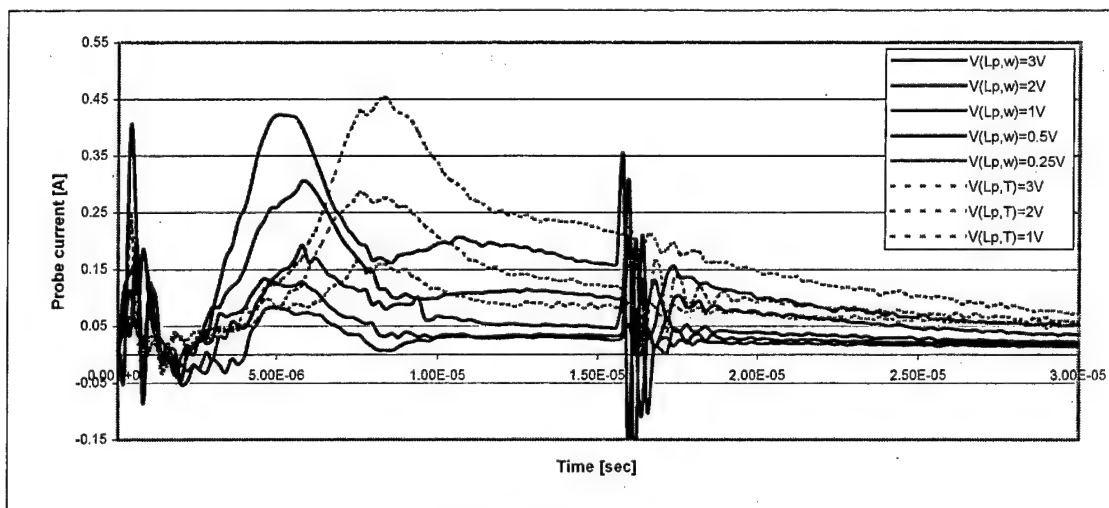


Fig. 9: Langmuir probe current for the Teflon<sup>®</sup> (dashed) and water mode (solid) and for different probe voltages at a location 11.4 cm downstream of the thrusters exit plane

#### Discussion of the experimental results

Different types of measurements showed clear indications that water is utilized in the discharge of the pulsed plasma thruster. Time of flight measurements showed exhaust velocities more than twice as high when water was introduced into the discharge compared to the ones achieved

with standard Teflon<sup>®</sup> propellant. This result is indicative of the reduced average molecular weight in the plasma plume. However, the gain in exhaust velocity is still smaller than the predicted one based on the comparison of the average mol weight (31 g/mol for Teflon<sup>®</sup> and 6 g/mol for fully ionized water). The reason for this observation is two folded: (i) The plasma



consists of a mixture of water and Teflon<sup>®</sup>, thereby increasing the average particle weight compared to its theoretical limit and reducing the average exhaust velocity and (ii) the discharge currents decrease significantly when water is fed into the thruster, decreasing thereby the electromagnetic contribution to the acceleration significantly.

The cause for the decrease of discharge peak currents is still investigated. It can be only partially explained by an increase of the time varying inductance due to the increase in plasma velocity. The initial assumption that not enough water is supplied and the discharge is starved is contradicted by the measurements shown in fig. 6. The amount of water participating in the discharge is still an unknown variable. The amount of vaporized water vapor between the electrodes actually might be too big, therefore increasing the plasma resistance. Another possibility might be that some properties of the water itself cause the increase of the plasma resistance. It is well known that in air for certain conditions the presence of water vapor can for example significantly increase the breakdown threshold.

The higher electron temperature in case of the water mode is a further indication of the existence of water in the thruster plume, even though the difference between the water mode (3.2eV) and the Teflon<sup>®</sup> mode (2.6eV) is too small to allow further interpretations.

### Conclusion

A simple and robust water feed system for a Pulsed Plasma Thruster was designed, built, and tested. The configuration utilized for the present paper results in a plasma composed of dissociation products of Teflon<sup>®</sup> and water. Time of flight measurements showed an increase of exhaust velocities of a factor 2 when water is added to the Teflon<sup>®</sup> compared to a case where only Teflon<sup>®</sup> is present. Furthermore, the addition of water causes a slight increase of measured electron temperature. Measurements of the discharge

currents showed an increase in both, plasma inductance and resistance. The reason for this phenomenon is still under investigation. A separated experiment has been designed and built to support the search for suitable media, which can be used for the water feed system. However, further efforts, both theoretical and experimental have to be made to better understand the water transport in the diffusion media. This is especially important with regard to the amount of water, which is available at the time of discharge initiation since this might give insight into the dominant plasma processes and therefore explain the observed reduction of the discharge current.

### Acknowledgements:

This work was supported by the Air Force grant No. F49620-00-1-0032. The authors acknowledge the help and support of Hani Kamhawi and Eric Pencil from NASA Glenn Research Center.

### References

- [1] D.J. Palumbo, W.J. Guman, "Effects of Propellant and Electrode Geometry on Pulsed Ablative Plasma Thruster Performance", J. of Spacecraft, Vol.13, No. 3, March 1976
- [2] R.J. Leiweke, P.J. Turchi, H. Kamhawi, R.M. Myers, "Experiments with Multi-Material Propellants in Ablation-Fed Pulsed Plasma Thrusters", AIAA 95-2916
- [3] E.J. Pencil, H. Kamhawi, L.A. Arrington, W.B. Warren, "Evaluation of Alternate Propellant for Pulsed Plasma Thruster", IEPC-01-147, 27<sup>th</sup> IEPC, 2001
- [4] C.A. Scharlemann, R. Corey, I.G. Mikellides, P.J. Turchi, P.G. Mikellides, "Pulsed Plasma Thrusters Variations for Improved Mission Capabilities", AIAA-00-3260, 36<sup>th</sup> AIAA Joint Propulsion Conference, July 2000, Huntsville, Alabama
- [5] J. K. Ziemer, R. A. Petr, "Performance of Gas Fed Pulsed Plasma thrusters Using water Vapor Propellant, AIAA-2002-4273, JPC, July 2002
- [6] J.K. Ziemer, T.E. Markusic, E.Y. Choueiri, D. Birx, "Effects of Ignition on Discharge Symmetry in Gas-Fed Pulsed

Plasma Thrusters" AIAA-98-3803, 34<sup>th</sup> JPC, July, 1998

[7] C.A. Scharlemann, T.M. York, P.J. Turchi, "Alternative Propellants For Pulsed Plasma Thrusters", AIAA-2002-4270, 38<sup>th</sup> AIAA Joint Propulsion Conference, July 2002, Indianapolis, Indiana

[8] H. Kamhawi, P.J. Turchi, R.J. Leiweke, R. M. Myers, "Design and Operation of a Laboratory Bench-Mark PPT", AIAA 96-2732, 32<sup>nd</sup> JPC, July 1996

[9] Effect of Propellant Temperature on Efficiency in the Pulsed Plasma Thruster, G.G. Spanjers, J.B. Malak, R. J. Leiweke, R.A. Spores, Journal of Propulsion and Power, Vol. 14, No. 4, July-August 1998

[10] L.T. Byrne, H.S. Seling, A.T. Wheelock, N.A. Gatsonis, E. J. Pencil, "Near Field Triple Langmuir Probe Measurements of a Pulsed Plasma Thruster in a Large Vacuum Facility", AIAA-2000-3258, IEPC, 2001

[11] F.F. Chen, "Plasma Physics and Controlled Fusion", 2<sup>nd</sup> ed., 1984 Plenum Press

[12] R. Huddelstone, S. Leonard, "Plasma diagnostic Techniques", Academic Press Inc., 1965

[13] M. Hirata and H. Murakami, "Exhaust Gas Analysis of a Pulsed Plasma Engine", IEPC 84-52, Tokyo, Japan, Sep. 1984





AIAA-2003-5022

**Pulsed Plasma Thruster Using Water Propellant,  
Part I: Investigation of Thrust Behavior and  
Mechanism**

Carsten A. Scharlemann  
The Ohio State University  
Columbus, OHIO

Thomas M. York  
The Ohio State University  
Columbus, OHIO

39<sup>th</sup> AIAA/ASME.SAE/ASEE Joint Propulsion Conference  
20-23 July 2003  
Huntsville, Alabama

For permission to copy or to republish, contact the copyright owner named on the first page.  
For AIAA-held copyright, write to AIAA Permissions Department,  
1801 Alexander Bell Drive, Suite 500, Reston, VA, 20191-4344.

# **PULSED PLASMA THRUSTER USING WATER PROPELLANT, PART I: INVESTIGATION OF THRUST BEHAVIOR AND MECHANISM**

**Carsten A. Scharlemann**  
The Ohio State University  
Department of Aerospace Engineering  
2300 West Case  
Columbus, OH 43235  
[scharlemann.1@osu.edu](mailto:scharlemann.1@osu.edu)

**Thomas M. York**  
The Ohio State University  
Department of Aerospace Engineering  
2300 West Case  
Columbus, OH 43235  
[york.2@osu.edu](mailto:york.2@osu.edu)

A water fed Pulsed Plasma Thruster offers a variety of advantages over the standard Teflon propellant. Experimental work, supported by numerical calculations, has shown that utilizing water results in an increased PPT performance and thereby broadens the range of mission applicability of PPTs. Furthermore, utilizing water offers the possibility of integration of PPT technology into In-Situ-Resource-Utilization mission and of reduced space vehicle contamination caused by the thruster plume. A simple and robust water propellant feed system is presented. The conceptual design of the propellant feed system is based on migration of the propellant through a suitable porous material. The sensitive issue of supplying the water at the right time to the main discharge was resolved by injecting the water mass bit together with the spark plug discharge. In the present paper a preliminary experimental investigation of this system is presented. Results from a PPT utilizing Teflon propellant are presented for comparison. Langmuir probe measurements indicate that in case of water the degree of ionization in the plume is much higher. Furthermore, measurements of the impact pressure in the plume of the PPT indicate a specific impulse several factors higher than achievable with Teflon.

## **Introduction**

Pulsed Plasma Thrusters are widely utilized due to their low power requirements, simplicity, and reliability. Their main task consists of north-south stabilization of satellites. However, the above listed attributes could also qualify them for future mission like visits to the outer regions of our solar system. But to be part of a future space exploration scenario it will be necessary to improve their performance with regard to their limited specific impulse and their low efficiencies.

One possibility to achieve these goals is the utilization of propellants other than the traditionally used Teflon<sup>®</sup>. Efforts to find a promising alternative to Teflon included LiOH seeded Teflon and different kind of thermoplastics like Halor, Tefzel<sup>1</sup>, variation of the ablative surface properties<sup>2</sup>, and Teflon of different densities, porosities, and level of carbon contains<sup>3</sup>.

Two years ago an effort to utilize water as propellant for PPTs was initiated at the Plasma Dynamic and Propulsion Laboratory of The Ohio State University. The advantages of water are numerous. Numerical simulations have shown a improvement in the thrust-to-power ratio<sup>4</sup>, water is nontoxic, it seems to be abundant in space (e.g. on comets or in the Jovian system etc.), it might reduce plume contamination, and it can be shared with other systems like life support systems or the main propulsion system (for example in case of a NERVA type main propulsion system) - to name only some of the most important advantages.

Main objective of this research was to develop a propellant feed system, which preserves the inherent simplicity of PPTs. In particular, it was aimed to avoid the complicated process of timing the propellant delivery with the discharge initiation - a problem, which cannot be avoided when using valves of any kind. An investigation into a passive water feed system was initiated. The philosophy here was to supply water into the vicinity of the discharge by allowing the water to diffuse through a porous material<sup>5</sup>. The mass flow rate of such a system is in a first approximation governed by Darcy's law:

$$\dot{m} = \rho \cdot k \cdot A \cdot \frac{dp}{dl} \quad (1)$$

with the density  $\rho$  (kg/m<sup>3</sup>) of water, the coefficient of permeability  $k$  (ms/kg), the cross sectional area  $A$  (m<sup>2</sup>) of the flow and the pressure gradient over the length of the diffusion head  $dp/dl$  (N/m<sup>3</sup>m). All the variables in eq. (1) are easily adjustable which allows good control of the mass flow rate over a large range. Various porous materials, including ceramics with different porosities, were investigated. Mass flow rates between 1 and 800  $\mu\text{g/s}$  were obtained by varying the thickness  $l$  and the contact surface  $A$  between water and the porous material. Subsequently a thruster was designed and built to verify the feasibility. Successful test were conducted and it was shown that indeed the thruster was using the supplied water. Additionally higher exhaust velocities were observed with water compared to the Teflon propellant<sup>6</sup>. However, one major concern was the relative high water mass flow rate necessary to

sustain the discharge. This resulted in large losses of propellant between two discharges. It was decided to initiate a complete redesign. The present paper focuses on this new design and initial experiments to investigate the differences between a PPT using water vs. one using Teflon.

#### Thruster and propellant feed system design

The new design conserves the philosophy of a passive propellant feed system. The water diffuses in a constant mass flow rate through a porous ceramic piece (COTRONICS 902) into the thruster. However, instead of supplying the water into the volume between the electrodes of the thruster as it was done before, it is now fed into a small volume in front of the spark plug (see figure 1).

A certain amount of water is stored in the structure of the porous ceramic piece, while a small amount lingers in the volume in front of the spark plug.

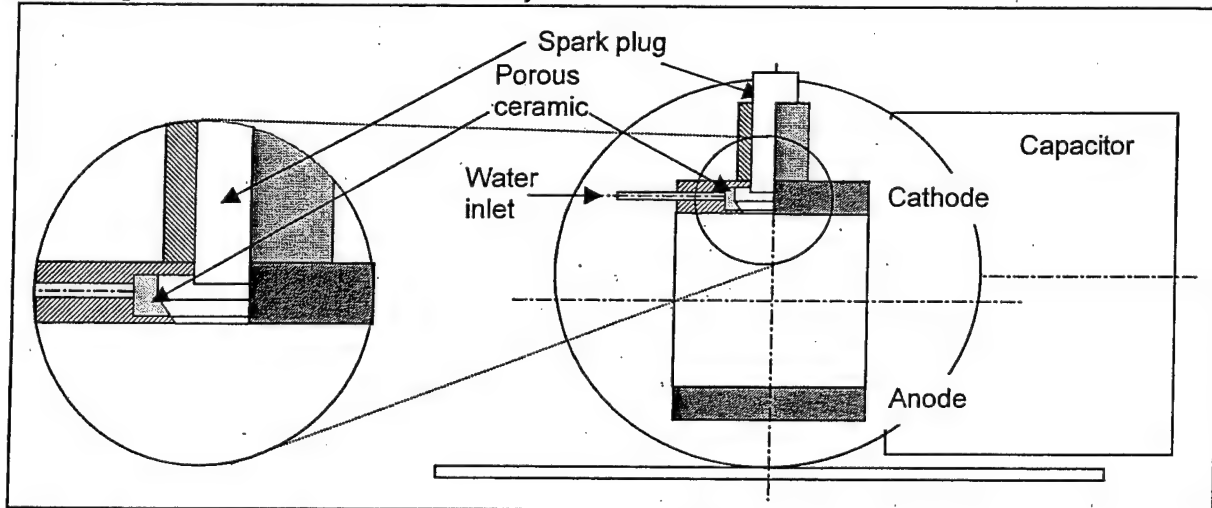


Fig.1: Front view of the water PPT with details of the water fed system

The rest escapes through the small slit into the area between the electrodes and subsequently into the vacuum chamber. When the spark plug is triggered it's discharge pushes the water out of the volume into the region between the electrodes where it initiates the main discharge. In this process it will be ionized and accelerated out of the thruster. By following this scheme, the major challenge of supplying the water propellant exactly at the time when the discharge is initiated has been circumvented. Additionally the possibility of a pre-ionization of the water by the spark plug itself exists. However further investigation have to be conducted in order to resolve this issue.

The water is stored in a small reservoir under atmospheric pressure. The reservoir itself is together with the thruster located inside the vacuum chamber. The thruster design is identical with the one recently reported<sup>5,6</sup>. It's design is such that it can also operate with Teflon propellant simply by removing the

cathode with the water feed mechanism and replace it with a standard cathode. When the thruster is used in the water mode, the Teflon block is replaced with a Boron Nitride plate.

#### Thruster operation

The experimental apparatus utilized for this work has been described in the literature before<sup>5</sup> and only the main features will be mentioned here again.

The vacuum system consists of a roughing pump in conjunction with a turbomolecular pump and allows to reach background pressures of around  $2 \times 10^{-5}$  Torr in a relative short time. The discharge current in a PPT does change with changing background pressures. This is mainly – but not only – a function of the number density or air molecules present between the electrodes. The magnitude and shape of the discharge current has a strong influence on the thruster performance in particular on the Teflon

ablation rate. In order to compare different thruster configurations with each other they should be conducted at roughly the same background pressures. Due to the different molecular weight of water compared with the average molecular weight of air, the pressure readings will differ when the thruster operates in the water mode. To accommodate this fact, a correction factor  $\xi = 0.891^7$  (1mTorr air pressure corresponds to 0.891 mTorr water pressure) for the ion gauge reading is necessary. With a background pressure for the thruster tests with water of  $1.1 - 1.2 \times 10^{-4}$  Torr and for the tests with Teflon of  $7.5 - 9.0 \times 10^{-5}$  Torr acceptably close conditions were obtained.

For both cases, water and Teflon, the discharge frequency was chosen to be  $1 \text{ Hz} \pm 2\%$ . The thruster is equipped with a  $30 \mu\text{F}$  capacitor (Maxwell Laboratories Inc.) with a 2 kV rating and a maximum peak current of 25 kA. The capacitor is charged up to 816 V, 1150 V, and 1414 V equivalent to discharge energies of roughly 10J, 20J, and 30 J.

#### Discharge current and voltage

During thruster operation the discharge current and voltage were monitored. For the latter a standard voltage probe (Tektronix P5100,  $\times 100$ , 2.5kV peak) was utilized to measure the voltage across the capacitor. The discharge current was measured by a

house made Rogowsky coil, which was calibrated with a Pearson Current monitor #5046. The Rogowsky coil is attached around the hot stud of the capacitor and is connected to the oscilloscope via a RC integrator.

A comparison for the discharge currents and capacitor voltages when using Teflon vs. water is depicted in Fig.2 and 3. The well known shot-to-shot variation in terms of the peak current is in both case relative small ( $\pm 1.5\%$  for Teflon and  $\pm 2.5\%$  for water). On the other hand, the variation in onset of the discharge current is for water roughly  $\pm 0.5 \mu\text{s}$  while negligible for Teflon. To cope with these variations an averaging method was applied. Each curve shown in fig. 2 and 3 represents the arithmetic average of 5 single measurements as mentioned above.

It is evident from fig.2 that in case of water the peak discharge currents are smaller, the discharge is more prolonged, and the period  $T$  is longer. This is also mirrored by the result of an analysis of the discharge current with regard to the circuit parameters: while the inductance  $L$  and resistance  $R$  for the Teflon case are relatively small with  $L=54 \text{ nH}$  and  $R= 13.1 \text{ m}\Omega$ , they are much higher for water with  $L=91 \text{ nH}$  and  $R= 35 \text{ m}\Omega$  respectively.

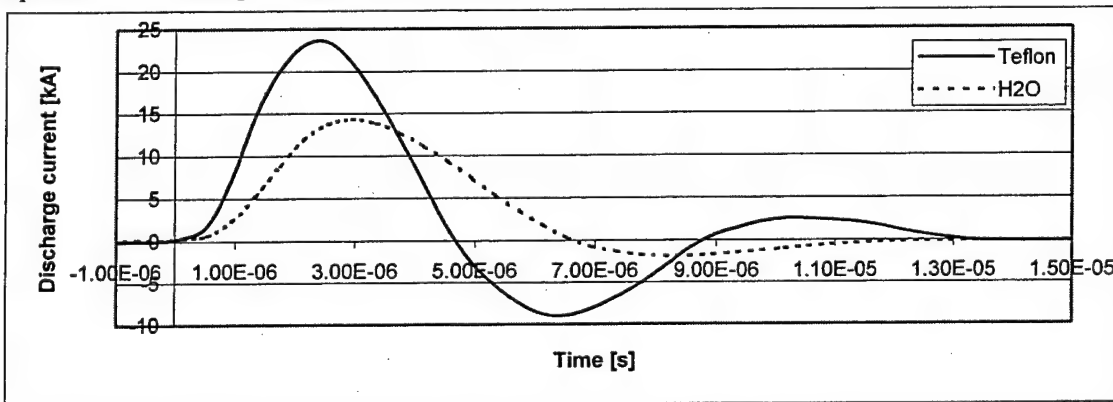


Fig 2: Comparison of discharge currents for Teflon and water propellant (30 J)

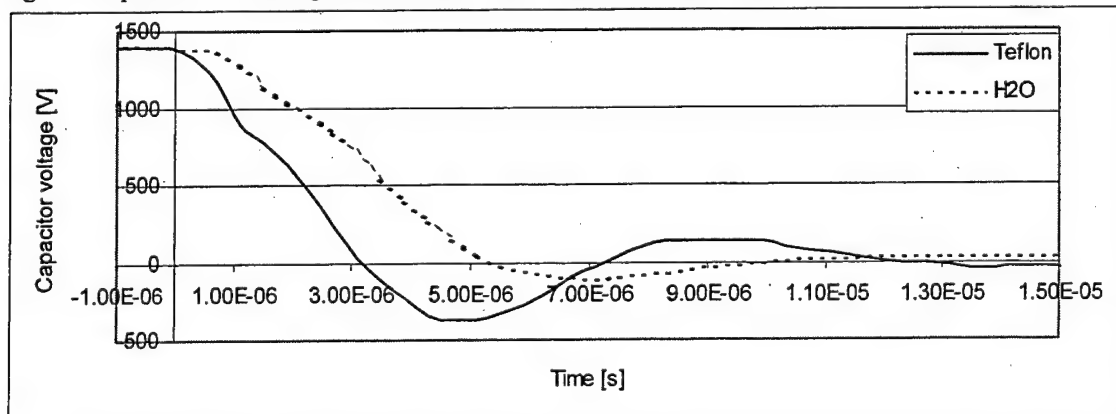


Fig.3: Comparison of capacitor voltage history during a discharge for Teflon and water propellant (30 J)

### Mass consumption

The Teflon utilized was a standard type with a density of roughly  $1.98 \times 10^3 \text{ kg/m}^3$ . In case of the water tests, a pyrex re-distilled water was used to keep the percentage of impurities low (total organic carbon: 1.8 mg/L, total silica: 1.1 mg/L, chlorides: 1 mg/L).

Due to the different ways of supplying the propellant to the discharge, two different methods to evaluate the mass consumption were utilized and are described in the following:

#### A: Teflon

In case of Teflon, a simple weight measurement is sufficient. The mass consumption in the Teflon mode was evaluated by measuring the weight of the Teflon bar ( $\sim 2.54 \times 2.54 \times 2.54 \text{ cm}$ ) before and after a run (Mettler AE100).

The mass bits were evaluated for 10, 20, and 30 J discharge energy. For all discharge energies, the thruster was operating for  $>5000$  discharges. Since the temperature was not monitored for these runs and in order to avoid excessive heating of the thruster, all the runs were split into two with a 1 hour break between them (2 hours in case of the 30 J test). Table 1 summarizes the ablation results. After the conclusion of the run the Teflon bar was kept in an acclimatized room where it was allowed to adjust to the humidity of the environment for 24 hours before it's weight was measured.

The results are typical for a PPT of this kind with the exception of the 10 J case. In the 10 J case a slight carbonization of the Teflon ablation surface was observed. This is assumed to be the reason for the unusual low ablation rate at this energy level.

Table 1: Teflon ablation rates for various discharge energies

Discharge energy [J]	# of discharges	Ablation/discharge [ $\mu\text{g}$ ]	Ablation/unit of energy [ $\mu\text{g/J}$ ]
10	5400	11.9	1.19
20	5400	27.5	1.375
30	5500	35.3	1.18

#### B: Water

The water consumption rate per discharge are evaluated based on the pressure rise in the closed vacuum chamber. For these mass flow tests, the experimental setup is slightly changed. Instead of having the water stored in a reservoir inside the vacuum chamber, it is now located outside the vacuum chamber and connected through a pipe to the ceramic diffusion disk inside the chamber. An electromagnetic valve separates the water reservoir from the vacuum chamber. The pressure driving the mass flow is about the same as in the thruster experiments, namely one atmosphere.

Prior to the mass flow rate measurement, the vacuum chamber was pumped down for a period of 28 hours. After this time the main gate valve, separating the vacuum chamber from the pump system, was closed and the pressure rise in the vacuum chamber over time ( $dp/dt$ ) was monitored (in this phase the pressure rise is due mainly to vacuum chamber leaks). The mass flow rate of air  $\dot{m}_{\text{air}}$  causing the pressure rise can be approximated by

$$\dot{m}_{\text{Air}} = \left( \frac{dp}{dt} \right) \frac{V_c}{R_{\text{Air}} \cdot T} \quad (2)$$

with the specific gas constant  $R_{\text{Air}}$  ( $287 \text{ J/(kgK)}$ ) and the temperature  $T$  (assumed to be room temperature,  $\sim 300 \text{ K}$ ).

After the pressure in the chamber has reached 20 mTorr, the electromagnetic valve was opened, allowing the water to get in contact with the porous ceramic and diffuse through it into the vacuum chamber. The measured  $(dp/dt)'$  is now the sum of the above discussed leakage of air  $\dot{m}_{\text{air}}$  and the additional water mass flow rate  $\dot{m}_{\text{H}_2\text{O}}$  into the chamber (see fig.4). The latter can be evaluated with eq. 3:

$$\dot{m}_{\text{H}_2\text{O}} = \left( \left( \frac{dp}{dt} \right)' \frac{V_c}{R_{\text{H}_2\text{O}} \cdot T} \right) - \dot{m}_{\text{Air}} \cdot \frac{R_{\text{Air}}}{R_{\text{H}_2\text{O}}} \quad (3)$$

with  $R_{\text{H}_2\text{O}} = 461 \text{ J/kgK}$ .

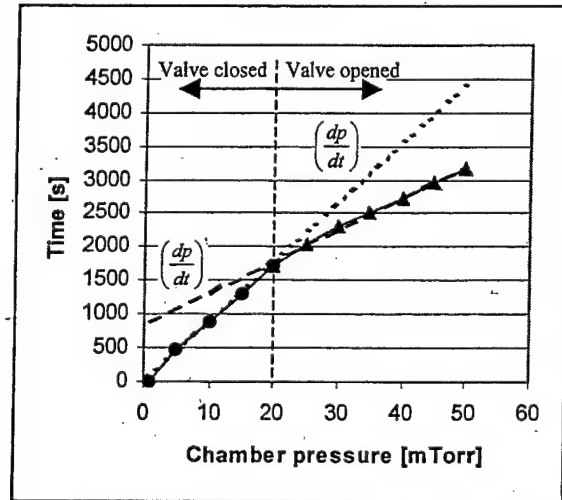


Fig.4: Evaluation of the water mass flow rates (dashed lines are line fits to the experimental data of  $(dp/dt)$  and  $(dp/dt)'$ )

Analyzing the data depicted in fig.4, a water mass flow rate of  $1.1 \mu\text{g/s}$  is calculated. Since the above described mass flow measurement is conducted under the same conditions as all the experiments described here and in part II, the water mass flow rate of

1.1 $\mu$ g/s was assumed to be the water consumption during the experiments.

### Langmuir probe

Langmuir probes were used in the past to measure the electron temperature and density of a Teflon thruster in comparison with a water thruster<sup>6</sup>. However, the purpose of the Langmuir probe measurements for the present paper was to investigate qualitatively the difference between a PPT operating with water compared to an operation with Teflon. The utilized system consists of a double Langmuir probe, a supporting floating probe circuit and an oscilloscope (Tektronix, TDS 420A).

The Langmuir probe itself consists of two probe elements made of 0.127 mm diameter tungsten wire with an exposed surface length of 1 cm. The two tips are separated by a distance of 5 mm. The probe circuit keeps the tips of the probe on a certain voltage potential during a measurement. When the tips get in contact with the plasma ejected by the thruster, a current between the two tips will develop. For a given probe geometry the magnitude of this current is only a function of the state of the plasma and the applied voltage difference. This current is measured by a Tektronix probe current (P6021), which is connected between the probe circuit and the oscilloscope.

To minimize distortion of the current signal, the probe tips were frequently cleaned through electrical

means (glow cleaning). The glow cleaning circuit consists of a high voltage power supply (Keithley Instruments, #246) connected to the probe via a 100 k $\Omega$  resistor to avoid excessive currents in the cleaning circuit. By applying a voltage difference of around 500 V to the tips of the probe a small current between the two tips is generated, which – by means of ion bombardment – then cleans them. The polarity of the probe was switched several times to assure that both tips are evenly clean. For this process it was not required to open the vacuum chamber, however to be effective it was necessary to allow the pressure in the vacuum chamber to rise up to about 300-500 mT.

Fig.5 compares the probe signals obtained for the different midi (water vs. Teflon). Each sub figure includes two measurements for different locations downstream of the thruster. The voltage potential of the Langmuir probe was 3 V for all the measurements in fig.5.

Immediately recognizable is the far stronger signal for the water propellant. At the 2.54 location it's peak magnitude is more than 700% higher than the respective Teflon signal. This result is especially intriguing in connection with the above discussed much lower discharge currents. However, while the signal strength in case of Teflon only slowly weakens with increasing distance to the thruster, the water signal vanishes totally beyond a distances of 7 cm (for a probe potential of 3V).

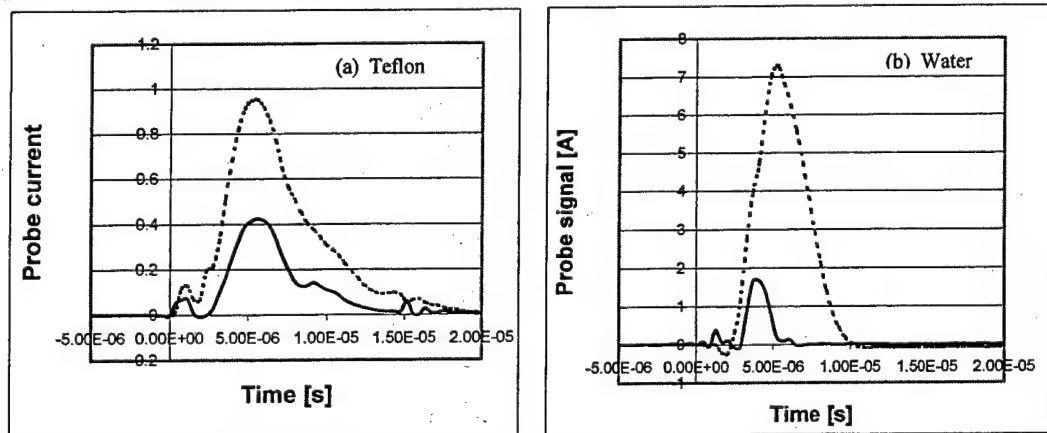


Fig.5: Comparison of the history of the Langmuir probe signal for Teflon and water at 2.54 cm (dashed line) and 5.04 cm (solid line) downstream of the thrusters exit plane

The higher Langmuir probe currents are indicating a higher degree of ionization of the water propellant compared to Teflon. This is partially due to the fact that more energy can be utilized for ionization processes rather than being deposit in vaporization and decomposition as it is in the case of Teflon. Additionally, the discharge in the water case is supplied with less material, therefore decreases the plasma densities and increases the ionization probability. It is also interesting to note that the probe

signal in the case of water is more defined and has a shorter duration than the respective signal for the Teflon mode.

### Pressure probe

Pressure probes are measuring the momentum flux of particles in general and are not restricted to charged particles the way Langmuir probes are. Therefore they open up the possibility to investigate the mass flow as a function of time with the potential to



explain the critical question of late time mass losses in a PPT. However, for the present paper the pressure probe measurements are mainly utilized to investigate qualitatively the differences between a PPT using Teflon vs. water. The probe signal for the high velocity and density of the exhaust flow is equal to the sum of the static and the dynamic pressure and can be expressed in the following way:

$$P_{\text{impact}} = P_{\text{static}} + P_{\text{dynamic}} \\ = (n_h + n_e) \cdot k \cdot T_e + n_h \cdot m_i \cdot u_{\text{exit}}^2 \quad (4)$$

with the heavy particle density  $n_h$  and the electron density  $n_e$  assumed to be equal (quasi neutral plasma), the electron temperature  $T_e$ , the average mass of the ions  $m_i$  and their exhaust velocity  $u_{\text{exit}}$ .

The here presented pressure probe was designed and utilized originally for MPD experiments<sup>8,9</sup>. The probes were designed to withstand the relative extreme conditions of a plasma environment (thermal loads and electromagnetic noise) and to have a high frequency response. The core of the pressure probe is a disk of piezoceramic material (PZT-5A) mounted to a backing rod with a conducting epoxy (see Fig.6). The disk and the backing rod are encased in a conducting shell, separated by a mylar foil around the circumference to prevent electric contact with the piezoceramic disk. The necessary electric contact between the front of the piezoceramic disk and the conducting shell is provided by a thin layer of silver paint. The whole unit is placed in a quartz tube, which has a flat fused end. A coax cable provides the electric contact to the electronic circuitry outside the quartz tube.

The quartz tube provides electric and thermal protection and at the same time allows stress waves to be transmitted to the piezoceramic disk.

In the occurrence of pressure, a charge difference builds up across the element and is manifested as a voltage transmitted through the connecting coaxial cable to an amplifier and a line follower. The amplifier and the line follower were built to match the output of the probe and allow the charge signal to be transmitted to an oscilloscope as an amplified voltage signal.

It is well known that the plume of a PPT consist of a initial front consisting of ionized particles possessing a relative high velocity. By impact on the pressure probe they induce strong stress waves into the probe, which initially drowned the pressure signal completely. A remedy was found by attaching a buffer on the front face of the probe. This buffer consists of a thin layer (~2mm) of soft plastic covered with a 1 mm thick ceramic disk in order to avoid ablation of the plastic. The buffer is attached onto the probe with a silicon glue.

Due to concerns about a possible deterioration of the buffer or the silicon glue a verification measurement was performed. After about a total of 6 hours of

usage of the probe, the probe was relocated to a former position and a measurement under the same conditions was performed. The results show no change with respect to the time of arrival or time of end of the signal and only marginal changes in the magnitude, which are well below the normal shot-to-shot variations.

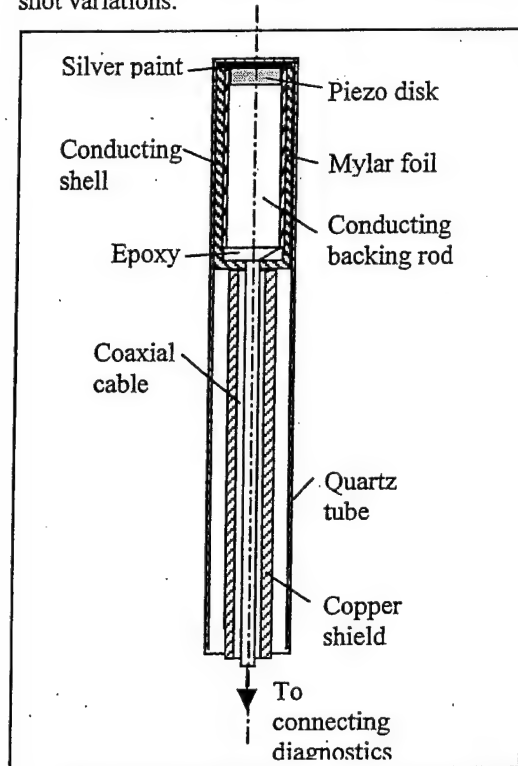


Fig.6: Cross Section of the pressure probe

#### Teflon

Before taking any measurements, the thruster was allowed to discharge for several minutes to avoid any transition effects. The shot-to-shot variations with regard to the discharge currents discussed above, can also be observed in the impact pressure measurements - although they are smaller than in the case of Langmuir probe measurements. However, in order to minimize the shot-to-shot variations, each graph presented in the following represents the arithmetic average of 5 successive measurements.

Pressure probes of this kind are charged coupled devices and therefore much more sensitive to electromagnetic noise than for example Langmuir probes. An additional potential source of noise is due to impact of parts of the plasma plume on the probe support. It is therefore important to conduct a noise investigation in order to distinguish noise from a signal due to impact on the sensing head of the pressure probe. This was done in regular periods and whenever the probe was relocated to a new position. In all the investigated case it was found that the noise is negligible compared with the main signal. The only exception is an initial peak (around 1-2  $\mu$ s into the

discharge) in the probe signal. It was found that the spark plug is the source of this noise signal.

Figure 7 shows the pressure probe signal for different discharge energies. Figure 8 depicts impact pressure measurements for the Teflon PPT at 3 different distances to the thruster's exit plane. As expected the magnitude of the signal decreases with increasing distances (the plume expands, resulting in a lower

momentum flux for locations further downstream), the onset of the signal happens later and the length of the signal increases with increasing distances ( $\sim 0.8\mu\text{s}$  longer for the 15.2 cm location compared to the 5.1 cm location).

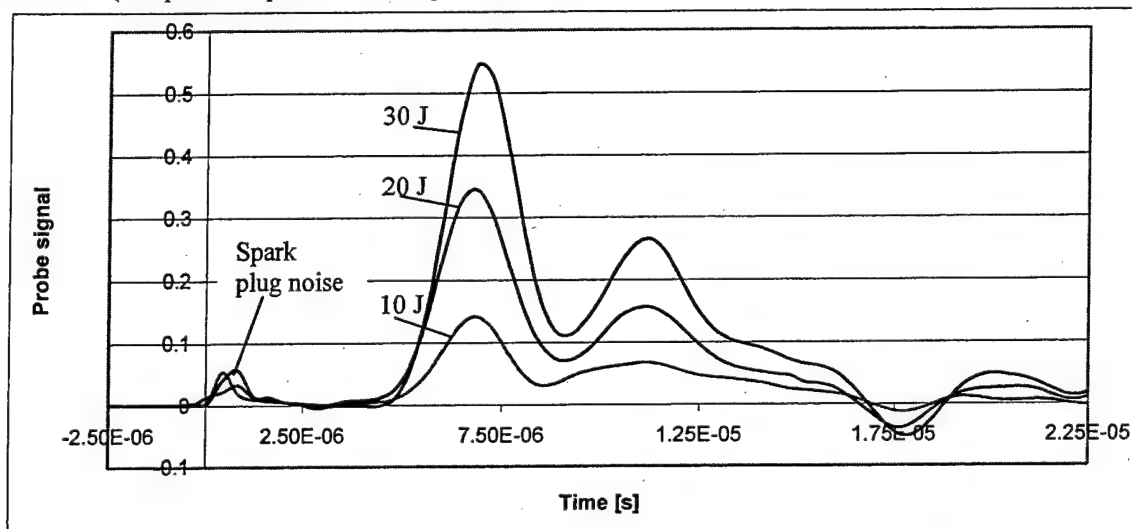


Fig. 7: Pressure probe signal for different discharge energies at 5.1 cm distance from the thruster's exit plane for PPT operating with Teflon

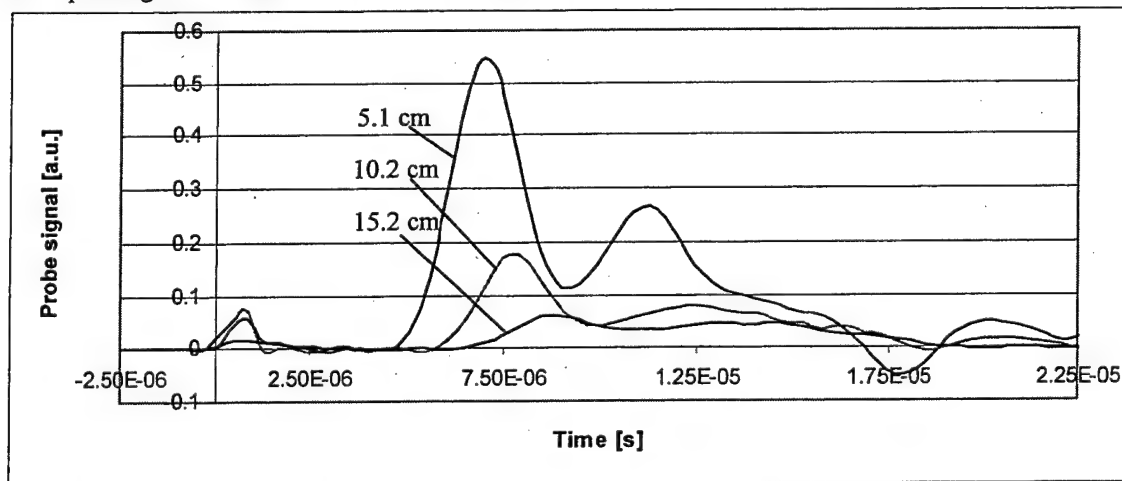


Fig. 8: Pressure probe signal at different distances for PPT operating with Teflon at 30 J

Similar to the results obtained with the Langmuir probe, the initial strong signal is followed by a weaker signal continuing for about  $10\mu\text{s}$ . It is interesting to note that for the same location, the onset of the pressure signal is delayed with respect to the onset of the Langmuir probe signal. This delay increases with increasing distance to the thruster indicating that two well distinguished particle fronts are observed: a initial plasma front consisting of mainly ionized particles with high velocity but relatively low density followed by a front of mainly

neutrals moving slower but exhibiting higher densities.

#### Water

The impact pressure measurements described above were repeated with water as propellant. Since the general trends are the same, the following paragraph focuses mainly on differences between the two propellants rather than following the same scheme as the paragraph above.

Figure 9 shows the two main differences between water and Teflon: (i) at the same downstream



location the onset of the signal for water happens earlier than for Teflon and the time difference increases with increasing distance to the thruster; (ii)

the signal strength for the Teflon propellant is larger than for water.

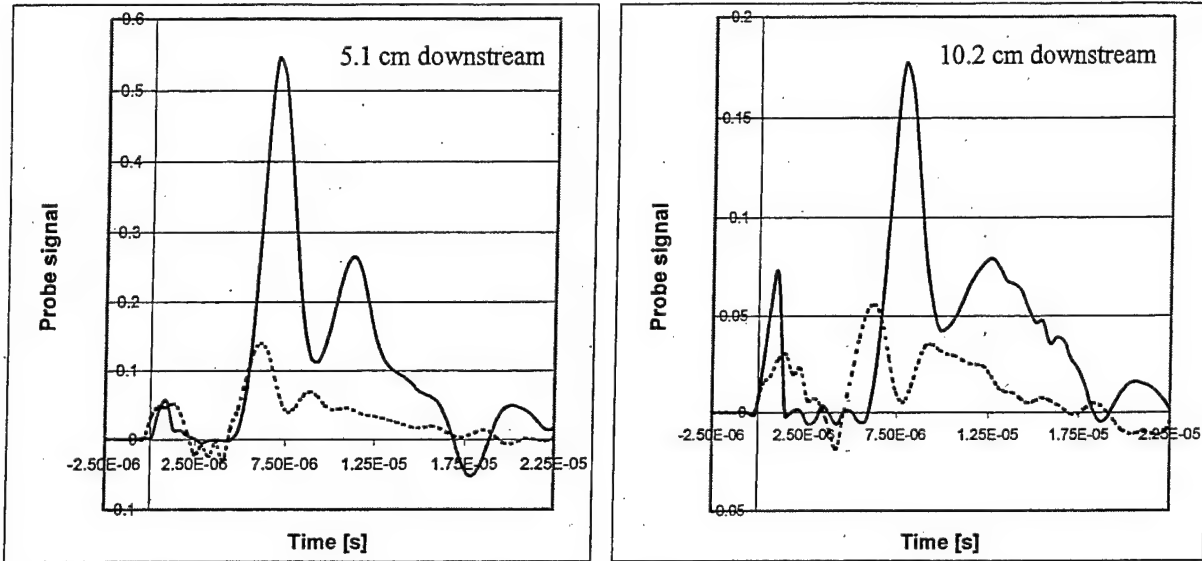


Fig.9: Comparison between the impact pressure signal when using water (dashed) vs. Teflon (solid) for two downstream locations (for 30 J discharge energy)

The plume of the PPT consists of particles with velocities varying over a large range. However in order to extract some information about the different velocities indicated in fig.9, a comparison of the times of the onset of the signal for different distances was conducted. Utilizing the data depicted in fig.9, a peak velocity of 46 km/s for the Teflon thruster is calculated. Repeating this calculation for water, results in a peak velocity of 127 km/s. The larger velocity for water is attributed to the lower average mol weight for water (6g/mol) compared to the average mol weight of Teflon (31 g/mol)<sup>10</sup> and the lower plasma densities. Note, that these higher velocities are obtained even though the discharge currents are much lower for water.

### Discussion

A simple water feed system was designed and tested. It is based on the diffusion of the water propellant through a porous ceramic piece, driven by the pressure difference between the water reservoir and the vacuum chamber. The water is supplied into a region close to the spark plug. When the spark plug discharges it feeds the water automatically into the volume between the thruster's electrodes where it initiates the main discharge. By applying this scheme any difficulties connected to the timely provision of the propellant to the discharge were circumvented. The water mass bits for the Teflon and water mode were evaluated. While the mass bits for Teflon are between 12  $\mu\text{g/s}$  and 35  $\mu\text{g/s}$ , the mass bit in the water mode is only 1.1  $\mu\text{g/s}$ . Similar to the Teflon PPT it is unknown yet how much of the water is actually used in the discharge. However, it is expected that the

losses are lower than in the case of Teflon due to the relative small size of the supplied propellant.

Monitoring the discharge currents for both modes it was observed that the peak discharge currents in the water mode are about 40% lower than in the Teflon mode. However, in spite of the lower discharge currents, preliminary measurements with a double Langmuir probe indicate a higher degree of ionization in the water plasma than it is the case for the Teflon mode. A possible explanation for this observation might be that the lower density of the water plasma allows a better ionization. Additionally, less energy is deposit into vaporization and decomposition of the water than it is the case for Teflon.

Impact pressure measurements in the plume of the thruster are used to identify further differences between the two modes; they indicate a more efficient acceleration process with the water plasma. Lower impact pressures were measured in the water mode than in the respective Teflon mode. This is related to the much smaller mass bits provided in the water mode. However, peak particle velocities in the water mode are nearly 3 times as high as the ones observed in the Teflon mode. The latter suggests a high specific impulse and higher thruster efficiency when operating with water propellant.

Further analysis of the data is necessary, especially focusing on a time resolved mass flow analysis in a PPT plume. This has the potential to provide a better understanding of the critical question of late time mass losses in PPTs. This analysis will be complemented by investigation of the plume with spectroscopic means.

### Acknowledgements

This work was supported by the Air Force grant No. F49620-00-1-0032.

### References

- [1] D.J. Palumbo, W.J. Guman, "Effects of Propellant and Electrode Geometry on Pulsed Ablative Plasma Thruster Performance", J. of Spacecraft, Vol.13, No. 3, March 1976
- [2] R.J. Leiweke, P.J. Turchi, H. Kamhawi, R.M. Myers, "Experiments with Multi-Material Propellants in Ablation-Fed Pulsed Plasma Thrusters", AIAA 95-2916
- [3] E.J. Pencil, H. Kamhawi, L.A. Arrington, W.B. Warren, "Evaluation of Alternate Propellant for Pulsed Plasma Thruster", IEPC-01-147, 27<sup>th</sup> IEPC, 2001
- [4] C.A. Scharlemann, R. Corey, I.G. Mikellides, P.J. Turchi, P.G. Mikellides, "Pulsed Plasma Thrusters Variations for Improved Mission Capabilities", AIAA-00-3260, 36<sup>th</sup> AIAA Joint Propulsion Conference, July 2000, Huntsville, Alabama
- [5] C.A. Scharlemann, T.M. York, P.J. Turchi, "Alternative Propellants For Pulsed Plasma Thrusters", AIAA-2002-4270, 38<sup>th</sup> AIAA Joint Propulsion Conference, July 2002, Indianapolis, Indiana
- [6] C.A. Scharlemann, T.M. York, "Investigation of a PPT utilizing water as component propellant", IEPC-03-112, IEPC 2003, Toulouse, France
- [7] Personal conversation with HELIX Technology Corporation
- [8] AIAA 71-196, "Pressure Measurements in the Exhaust Flow of a Pulsed Megawatt MPD Arc Thruster" C.J. Michels, T.M. York, Jan. 1971
- [9] "Stress Dynamics in High Speed Piezoelectric Pressure Probes", T.M. York, Review of Scientific Instruments, Vol.41, No. 4, April 1970, pp 519-521
- [10] M. Hirata and H. Murakami, "Exhaust Gas Analysis of a Pulsed Plasma Engine", IEPC 84-52, Tokyo, Japan, Sep. 1984



AIAA-2003-5023

**Pulsed Plasma Thruster Using Water Propellant,  
Part II: Thruster Operation and Performance  
Evaluation**

Carsten A. Scharlemann  
The Ohio State University  
Columbus, OHIO

Thomas M. York  
The Ohio State University  
Columbus, OHIO

39<sup>th</sup> AIAA/ASME.SAE/ASEE Joint Propulsion Conference  
20-23 July 2003  
Huntsville, Alabama

For permission to copy or to republish, contact the copyright owner named on the first page.  
For AIAA-held copyright, write to AIAA Permissions Department,  
1801 Alexander Bell Drive, Suite 500, Reston, VA, 20191-4344.

# **PULSED PLASMA THRUSTER USING WATER PROPELLANT, PART II: THRUSTER OPERATION AND PERFORMANCE EVALUATION**

**Carsten A. Scharlemann**  
The Ohio State University  
Department of Aerospace Engineering  
2300 West Case  
Columbus, OH 43235  
[scharlemann.1@osu.edu](mailto:scharlemann.1@osu.edu)

**Thomas M. York**  
The Ohio State University  
Department of Aerospace Engineering  
2300 West Case  
Columbus, OH 43235  
[york.2@osu.edu](mailto:york.2@osu.edu)

Utilizing water as propellant for a Pulsed Plasma Thruster promises various advantages such as improved performance, increased mission applicability, and a potentially decreased space vehicle contamination. A new Pulse Plasma Thruster has been designed, built, and tested. The thruster is designed such that operation with water and with Teflon is possible, thereby allowing a direct comparison between a standard Teflon PPT and a PPT operating with water. To feed the water into the thruster and at the same time to retain the inherent simplicity of Pulsed Plasma Thrusters, a simple and robust water feed mechanism was designed. The conceptual design of the propellant feed system is based on diffusion of the propellant through a suitable porous material and subsequently injection into the discharge area by means of the spark plug.

Impulse bit measurements of the thruster operating in Teflon mode were conducted using a microthrust stand at NASA Glenn Research Center. These measurements were compared with impulse bit measurements using a pressure probe. The very close fit between those measurements allowed a quantification of the expected impulse bit of the thruster operating in the water mode. Preliminary performance calculation for a water PPT indicate a specific impulse of up to 12,000 s at a thruster efficiency of more than 24%.

## **Introduction**

A utilization of water as propellant for Pulsed Plasma Thrusters (PPT) promises a variety of advantages. Numerical calculations predict higher thrust-to-power ratios than achievable with a standard Teflon thruster<sup>1</sup>, water is non-toxic and it is easy to store, even for long periods of time. It can be shared with other key systems, like life support system or the main propulsion system (Nerva etc.). Furthermore a PPT operating with water fits well in In-Situ-Resource-Utilization (ISRU) mission scenarios. At the Plasma Dynamic and Propulsion Laboratory of The Ohio State University an effort was initiated to design, build, and test a PPT utilizing water as propellant.

The present paper is the second part of two papers dealing with this system and mainly focuses on thruster performance.

The details of the water PPT have been discussed in part I and shall only briefly be reviewed here.

The thruster was designed such that it can operate with Teflon and with water<sup>2</sup>. To switch between these two propellants only minor modifications are necessary. When operating with Teflon the thruster resembles a standard rectangular PPT. The electrodes have a length, width and gap size of 2.54 cm. The Teflon is fed between the two electrodes and kept in position by a spring mechanism pushing the Teflon bar against a retaining shoulder in the anode. The main discharge is initiated by a spark plug located about 9 mm downstream (measured from the centerline of the spark to the Teflon ablation surface).

To feed water into the discharge a different system was utilized as described in details in part

I. In general, the water is diffusing in a constant flow rate through a porous ceramic piece into a small volume in front of the spark plug (see figure 1). A certain amount of water will be stored in the structure of the porous ceramic piece, while a small amount lingers in the volume in front of the spark plug. The rest will escape through the small slit into the area

between the electrodes and the vacuum chamber. When initiating the discharge of the spark plug, the water will be pushed out of the volume into the region between the electrodes where it initiates the main discharge. In this process it will be ionized and accelerated out of the thruster.

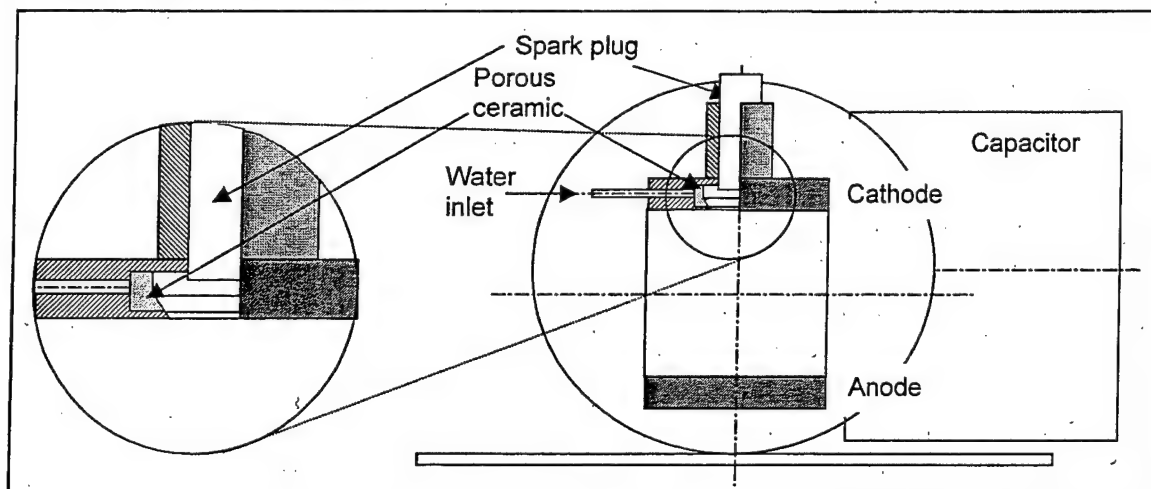


Fig. 1: Front view of the water PPT with details of the water fed system

#### Thruster operation

For both cases, water and Teflon, the discharge frequency was chosen to be  $1 \text{ Hz} \pm 2\%$ . As described in part I, the thruster was equipped with a  $30 \mu\text{F}$  capacitor (Maxwell Laboratories Inc.) with a 2 kV rating and a maximum peak current of 25 kA. The capacitor was charged up to 816 V, 1150 V, and 1414 V equivalent to discharge energies of roughly 10J, 20J, and 30 J. The discharge current in a PPT changes with changing background pressures. This is mainly, but not only, a function of the number density of molecules present between the electrodes. The magnitude and history of the discharge current has a strong influence on the thruster performance in particular the Teflon ablation rate. In order to compare different thruster configuration with each other they should be conducted at roughly the same background pressures. When the thruster is running with water, the residual gases in the vacuum chamber consist mainly of water molecules. Due to the different molecular weight of residue water compared with the average molecular weight of residue air, the ion gauge (Varian, type 0531) pressure readings will differ when the thruster operates with water. To accommodate this fact, a correction factor  $\xi = 0.891$  for the ion gauge reading is necessary<sup>3</sup> (1mTorr air pressure corresponds to 0.891 mTorr water pressure). Acceptable conditions were

obtained with a background pressure for the thruster tests with water of  $1.1 - 1.2 \text{ E-4 Torr}$  and for the tests with Teflon of  $7.5 - 9.0 \text{ E-5 Torr}$ .

#### Mass consumption

The details of the the mass consumption rate evaluation was described in part 1. In general, the mass consumption for the Teflon was evaluated by a simple measuring the weight of the Teflon<sup>®</sup> bar ( $\sim 2.54 \times 2.54 \times 2.54 \text{ cm}$ ) before and after a run with a Mettler AE100 weight balance (accuracy  $\pm 0.1 \text{ mg}$ ). The mass consumption was evaluated for 10, 20, and 30 J discharge energies and are summarized in table 1.

The results are in general typical for a PPT of this kind<sup>5</sup>. When the thruster was operating at 10 J a slight carbonization of the Teflon ablation surface was observed. This is assumed to be the reason for the too low ablation rate at this energy level.

Table 1: Teflon ablation results for various discharge energies

Discharge energy [J]	# of discharges	Ablation/discharge [ $\mu\text{g}$ ]	Ablation/unit of energy [ $\mu\text{g/J}$ ]
10	5400	11.9	1.19
20	5400	27.5	1.375
30	5500	35.3	1.18

Due to the different fashion how the water is supplied to the discharge, a different method to evaluate the water mass consumption was developed. The water diffuses through the porous ceramic in a constant mass flow rate. To measure the magnitude of it, a slightly different experimental setup is used. Instead of having the water stored in a reservoir inside the vacuum chamber, it is now located outside the vacuum chamber and connected through a pipe to the ceramic diffusion disk inside the chamber. An electromagnetic valve separates the water reservoir from the vacuum chamber. The pressure driving the mass flow is about the same as in the experiments, one atmosphere. During a period of 24 hours the vacuum chamber was pumped down. Subsequently the main gate valve, separating the vacuum chamber from the pump system, was closed and the pressure rise in the vacuum chamber over time ( $dp/dt$ ) was monitored. After a certain time, the above mentioned electromagnetic valve was opened, allowing the water to get in contact with the porous ceramic and diffuse through it into the vacuum chamber. The measured ( $dp/dt$ )' is now different due to the additional water diffusing into the vacuum chamber (see figure 2). By evaluating the difference between ( $dp/dt$ ) and ( $dp/dt$ )' a water mass flow rate of  $1.1 \mu\text{g/s}$  was calculated.

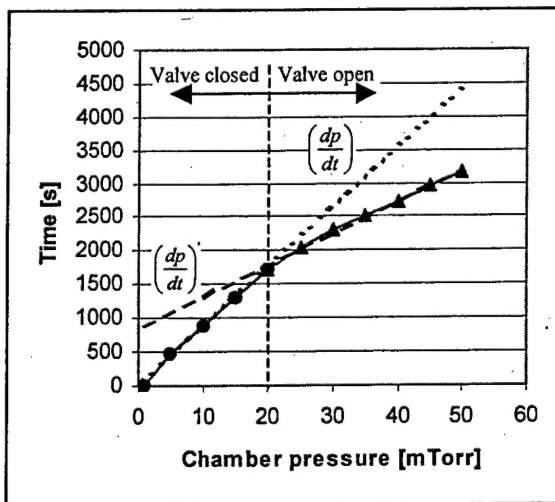


Fig.2: Evaluation of the water mass flow rates (dashed lines are line fits to the experimental data of ( $dp/dt$ ) and ( $dp/dt$ )')

#### Thruster impulse measurements

In the following impulse bit measurements made with a thrust stand at NASA Glenn Research Center (GRC) are correlated to the impulse bit measurements made with the pressure probes. The same Teflon thruster configuration was used for both types of measurements.

#### A: Impulse bit from thrust stand measurements

Impulse bit measurements were performed at NASA (GRC). A torsional-type thrust stand, located in a 1.5 m diameter by 4.5 m long oil diffusion pumped vacuum facility (VF-3) with a typical facility base pressure of  $2 \times 10^{-6}$  Torr (0.27 milliPa) was employed to measure the steady-state thrust and single impulse bit magnitudes for the PPT Teflon thruster<sup>4</sup>. The thruster configuration is identical to the one used in tests in the Plasma Dynamic and Propulsion Laboratory.

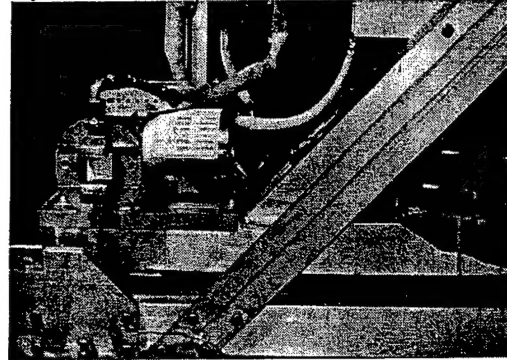


Fig.3: PPT installed on the thrust stand (note: no nozzle was used in these tests)

For the single impulse bit measurements, the reported values represent an average of ten pulses. The steady-state thrust was measured while the thruster was operating continuously for approximately five minutes at a frequency of 1.17 Hz. Single impulse bit and steady-state thrust measurements were performed for the PPT at energy levels of 10, 20, and 30 Joules. The results of these tests are summarized in table 2.

Table 2: Impulse bit results for the Teflon PPT measured at NASA Glenn Research Center

Discharge energy [J]	Impulse bit [ $\mu\text{N}\cdot\text{s}$ ]
10	122
20	273
30	440

#### B: Impulse bit from pressure probe measurements

For the present paper, the pressure measurements in the plume of the PPT were intended to investigate the difference between a water and Teflon thruster with regard to the impulse bit, exit velocity, efficiency etc. The details of those pressure probe measurements are described in part I.

The PPT plume is highly inhomogeneous in terms of number density, velocity etc. In order to obtain an accurate measurement of the impulse bit it would be theoretically necessary to conduct impact pressure measurements in a complete cross section

$A_{cs}$  of the plume. The probe signal for the high velocity and density of the exhaust flow is equal to the sum of the static and the dynamic pressure and can be expressed in the following way:

$$P_{impact} = P_{static} + P_{dynamic}$$

$$= (n_h + n_e) \cdot k \cdot T_e + n_h \cdot m_i \cdot u_{exit}^2 \quad (1)$$

with the heavy particle density  $n_h$  and the electron density  $n_e$  assumed to be equal (quasi neutral plasma), the electron temperature  $T_e$ , the average mass of the ions  $m_i$  and their exhaust velocity  $u_{exit}$ . To obtain the impulse bit  $I_{bit}$  the pressure probe output has to be integrated over the cross sectional area of the plume,  $A_{cs}$  and over time  $t$ .

$$I_{bit} = C \iint (p_{impact}) dt dA_{cs} \quad (2)$$

The constant  $C$  is attributed to various loss mechanism like thermal losses during the momentum transfer from the plasma to the probe, effects due to a possible shock in front of the probe, the general characteristic of the probe circuit (calibration constant of the probe was evaluated in the past by means of a shock tube), and differences in the vacuum facility (thrust stand tests and the pressure probe tests were done in different facilities). Determination of  $C$  is in general not trivial due to the various effects mentioned above. Additionally, in order to obtain good accuracy it would be necessary to conduct the impact pressure measurements at as many points as possible across a cross section  $A_{cs}$  of the plume. For the present paper a different method was chosen. Having the impulse bit measurements from NASA Glenn Research Center allows to simply correlate these results with the impact pressure measurements without being concerned about the losses mentioned above. Additionally, a comparison of the impact pressure measurements at one location on the thrusters axis for different discharge energies reveals a very convenient fact: By integrating the impact pressure signals obtained for 10, 20, and 30 J over the duration of the signal (see fig.5), it was found that their ratios constitute a very close match to the respective ratios of the impulse bit measurement results from NASA Glenn Research Center (as it should be since neglecting  $C$  and  $A_{cs}$  results only in a systematic error). Therefore one single pressure probe measurement in combination with the assumption that this pressure acts on average on a certain area, in the following called effective area  $A_{eff}$  (see fig.4), allows to obtain a good estimation for  $C$ .

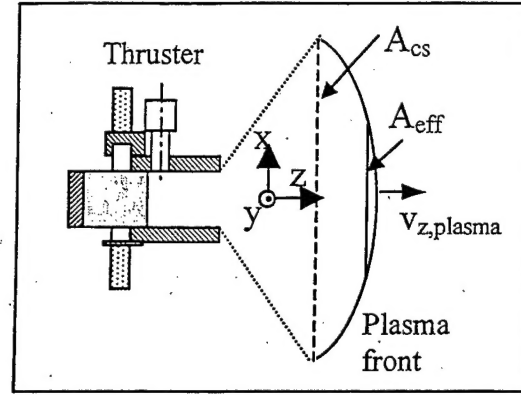


Fig. 4: Schematic of the expanding plasma front and the related areas

The effective area can be approximated with the knowledge of the extend the plasma front spreads out. Measurements of the impact pressure in the Teflon mode along the  $x$  and  $y$  axis at a distance of 5.02 cm were performed for this reason.

It was found that at a this distance the signal vanishes at around a  $(\pm x/\pm y)$ -location of  $(\pm 6\text{cm}/\pm 6\text{cm})$ , therefore indicating a total cross section  $A_{cs}$  of the plasma front of about  $150\text{ cm}^2$ . As a first approximation  $A_{eff}$  was defined to be equal to be  $80\text{ cm}^2$ . Utilizing eq. (2) and the results of the impulse bit measurements at NASA GRC, the preliminary value for  $C$  was evaluated to be equal to 10.2.

The process described above was performed for a discharge energy of 30 J. By having obtained  $C$  it is now possible to determine the impulse bit of other configurations or energies levels simply by measuring the impact pressure at the same location. The values for the Teflon and the water thruster obtained in such a fashion are given in table 3. A comparison of the such obtained impulse bit values with the ones measured at the NASA Glenn Research Center thrust stand (the (\*) marks the value which was used for evaluating  $C$ ) shows a very good fit. Furthermore, the table includes the impulse bit values for the water configuration solemnly based on the measurements of the impact pressure.



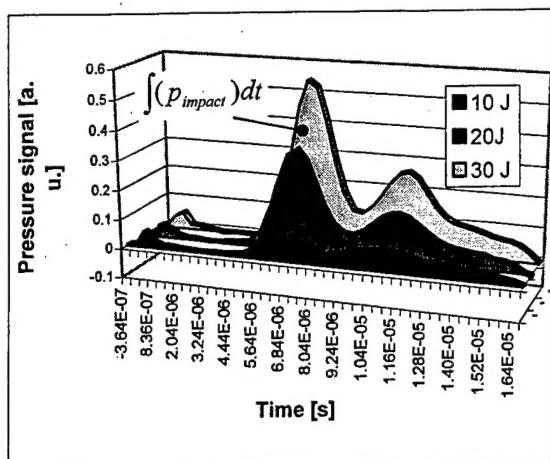


Fig. 5: Pressure probe signal for 10, 20, and 30 J discharge energy on the thrusters axis at 5.04 cm downstream (Teflon mode)

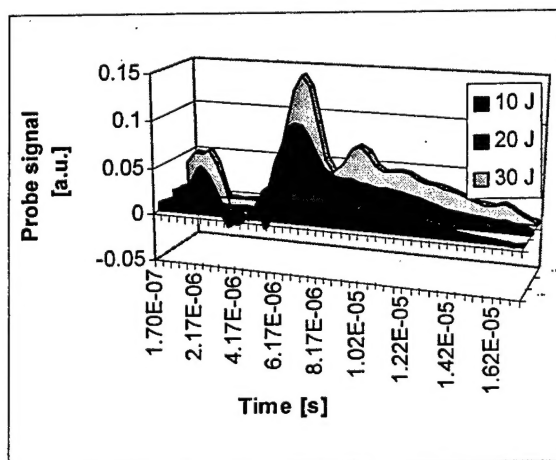


Fig.6: Pressure probe signal for 10,20, and 30 J discharge energy on the thrusters axis at 5.04 cm downstream (water mode)

### Performance

The performance calculations in the following have to be viewed as a preliminary result, conducted in order to understand trends rather than see the full potential of a water PPT. Based on the mass consumption measurements and the calibrated impact pressure measurements, described above, the following standard equations are utilized to calculate the specific impulse  $I_{sp}$  and efficiency  $\eta$ :

$$I_{sp} = \frac{I_{bit}}{\bar{m}_{loss} \cdot g} \quad (3)$$

$$\eta = \frac{I_{bit}^2}{2 \cdot E \cdot \bar{m}_{loss}} \quad (4)$$

With earth's gravitational acceleration  $g=9.81 \text{ m/s}^2$  and the discharge Energy  $E$ . The results of these calculations are summarized in table 3.

In general, the performance parameters for the thruster using Teflon compare well to similar thruster types like the LES-8/9 or the TIP-II (NOVA)<sup>5</sup>. The unusual low ablation rate for the 10 J case is attributed to an observed slight carbonization of the Teflon ablation surface.

The specific impulse and the efficiencies for water are several factors higher than for Teflon. This result is attributed to the lower average mol weight for water (6g/mol) compared to the average mol weight of Teflon (31 g/mol)<sup>6</sup> and the lower plasma densities. The latter is of course due to the low mass bits of the water thruster.

Table 3: Thruster performance for the water and Teflon mode

Discharge energy [J]	Impulse bit, GRC [ $\mu\text{N}\cdot\text{s}$ ]		Impulse bit, Pressure probe [ $\mu\text{N}\cdot\text{s}$ ]		Mass bit [ $\mu\text{g}/\text{discharge}$ ]		Specific impulse [s]		Efficiency	
	Teflon	Water	Teflon	Water	Teflon	Water	Teflon	Water	Teflon	Water
10	122	--	124	47	11.9*	~1.1	1060	4355	6.5	10
20	273	--	281	90	27.5	~1.1	1040	8340	7.2	18
30	440	--	440*	128	35.3	~1.1	1270	11860	9.1	24.8

### Discussion

Time of flight measurements in the plume of a water PPT suggested that much higher specific impulses can be obtained by utilizing water as propellant instead the standard Teflon propellant. In an effort to confirm these results, impact pressure measurements in the plume of the PPT using Teflon as propellant were performed. By

correlating these measurements with impulse bit measurements on a torsional-type thrust stand at NASA GRC it was shown that a very close fit between those two methods exists. This very close match allows to evaluate the impulse bit of a water thruster by measuring the impact pressure in the plume. It was indeed found that with such a thruster much higher impulse bits



and efficiencies can be obtained compared to a standard Teflon thruster.

However, this is considered to be a preliminary results since it is unknown yet if the correlation constant found for a thruster operating with Teflon can simply be transferred to the case of a water thruster. Effects like the different composition of the plasma (dissociated  $C_2F_4$  vs. water) might make it necessary to evaluate a different correlation constant. Further impulse bit measurements on the thrust stand at NASA GRC are therefore in preparation. These planned measurements will also include mass loss measurements at NASA GRC VF-3 to investigate facility effects on the mass loss magnitudes.

#### Acknowledgements

This work was supported by the Air Force grant No. F49620-00-1-0032. The authors acknowledge the help and support of Eric Pencil and Hani Kamhawi from NASA Glenn Research Center with the impulse bit measurements.

#### References

- [1] C.A. Scharlemann, R. Corey, I.G. Mikellides, P.J. Turchi, P.G. Mikellides, "Pulsed Plasma Thrusters Variations for Improved Mission Capabilities", AIAA-00-3260, 36<sup>th</sup> AIAA Joint Propulsion Conference, July 2000, Huntsville, Alabama
- [2] C.A. Scharlemann, T.M. York, P.J. Turchi, "Alternative Propellants For Pulsed Plasma Thrusters", AIAA-2002-4270, 38<sup>th</sup> AIAA Joint Propulsion Conference, July 2002, Indianapolis, Indiana
- [3] Personal conversation with HELIX Technology Corporation
- [4] Haag, T. W., "Thrust Stand for Pulsed Plasma Thrusters," *Rev. Sci. Instrum.*, 68 (5), 1997.
- [5] R.L. Burton, P.J. Turchi, "Pulsed Plasma Thruster", *J. of Propulsion and Power*, V.14, No.5, pp 716-735
- [6] M. Hirata and H. Murakami, "Exhaust Gas Analysis of a Pulsed Plasma Engine", IEPC 84-52, Tokyo, Japan, Sep. 1984